

Final-state rescattering mechanism of charmed baryon decays

Cai-Ping Jia^{*},¹ Hua-Yu Jiang[†],² Jian-Peng Wang[‡],¹ and Fu-Sheng Yu^{§1}

¹*MOE Frontiers Science Center for Rare Isotopes,
and School of Nuclear Science and Technology,
Lanzhou University, Lanzhou 730000, China*

²*Institute of Particle and Nuclear Physics,
Henan Normal University, Xinxiang 453007, China*

(Dated: August 28, 2024)

Abstract

The dynamical studies on the non-leptonic weak decays of charmed baryons are always challenging, due to the large non-perturbative contributions at the charm scale. In this work, we develop the final-state rescattering mechanism to study the two-body non-leptonic decays of charmed baryons. The final-state interaction is a physical picture of long-distance effects. Instead of using the Cutkosky rule to calculate the hadronic triangle diagrams which can only provide the imaginary part of decay amplitudes, we point out that the loop integral is more appropriate, as both the real parts and the imaginary parts of amplitudes can be calculated completely. In this way, it can be obtained for the non-trivial strong phases which are essential to calculate CP violations. With the physical picture of long-distance effects and the reasonable method of calculations, it is amazingly achieved that all the nine existing experimental data of branching fractions for the Λ_c^+ decays into an octet light baryon and a vector meson can be explained by only one parameter of the model. Besides, the decay asymmetries and CP violations are not sensitive to the model parameter, since the dependence on the parameter is mainly cancelled in the ratios, so that the theoretical uncertainties on these observables are lowered down.

PACS numbers:

^{*} jiACP20@lzu.edu.cn, corresponding author
[†] jianghuayu@htu.edu.cn, corresponding author
[‡] wangjp20@lzu.edu.cn, corresponding author
[§] yufsh@lzu.edu.cn, corresponding author

Contents

I. Introduction	2
II. Theoretical Framework	4
A. Topological diagrams and non-perturbative contribution	4
B. Short-distance contributions with factorization hypothesis	5
C. Long-distance contributions with final-state rescattering mechanism	7
III. Analytical discussions	12
A. Cutkosky cutting rule and Feynman loop integral	12
B. Pauli-Villars regularization and model form factors	13
IV. Numerical results and discussion	14
A. Inputs	14
B. Branching ratios	15
C. Decay parameters	18
D. CP asymmetries	19
V. Summary	21
Acknowledgments	22
A. Amplitudes of each modes	22
1. Cabibbo-favored	22
2. Singly Cabibbo-suppressed	23
3. Doubly Cabibbo-suppressed	24
B. Effective Lagrangian	24
References	24

I. INTRODUCTION

In the non-leptonic weak decays of heavy flavour hadrons, the effects of long-distance or soft QCD dynamics are important for generating strong phases, which are essential component of the direct CP violation mechanism. CP asymmetry is sensitive to strong phases and is a necessary condition for understanding the matter-antimatter asymmetry in our universe [1]. However, there is no appropriate QCD-based approach for calculating the long-distance contributions due to the large soft-overlap effects of initial and final states. The QCD factorization (QCDF) [2–5] and perturbation QCD (PQCD) [6–8] approach are mainly employed to calculate the contributions with small soft-overlap effects of hadron wave functions. Therefore, it is crucial to build up an appropriate framework for estimating the long-distance non-perturbative effects in heavy flavour hadron decays. In this work, we take the two-body non-leptonic decays of charmed baryons as the starting point to study the long-distance non-perturbative dynamics and improve the calculation method that can reasonably describe the effects of the final-state interactions.

a lot of experimental measurements on the charmed baryon decays have been performed during the past decade [9–75]. The BESIII and Belle (II) experiments have measured the branching ratios and decay asymmetry parameters for a large amount of non-leptonic decay channels of charmed baryons. Besides, the most precise measurement on the CP violation in charmed baryon decays up

to date is given by LHCb as $A_{CP}^{dir}(\Lambda_c^+ \rightarrow pK^+K^-) - A_{CP}^{dir}(\Lambda_c^+ \rightarrow p\pi^+\pi^-) = (0.30 \pm 0.91 \pm 0.61)\%$ [10]. Decay asymmetry parameters and CP violation are of particular interest because they are sensitive to the strong phases in the decay and provide stronger constraints for theoretical analysis. More experimental results will be forthcoming with even larger data samples collected by BESIII, Belle II and LHCb in the near future. Therefore, the corresponding theoretical studies are urgently needed to understand the dynamics of charmed baryon decays and to accurately calculate the relevant observables.

The study of charmed baryon decays faces a lot of theoretical challenges, due to insufficient understanding of complicate dynamics in baryon system and non-perturbative dynamics at the charm scale. From 1990s to now, there are many theoretical attempts to study the non-leptonic decays of charmed baryons [76–111]. The most widely used analysis method is based on the flavor $SU(3)$ symmetry method, combined with an extensive global fit to the experimental data, which does not provide enough information of the decay dynamics. Compared with the case of charmed mesons, there are many more non-perturbative parameters that need to be fitted in the charmed baryon decays, which makes it currently mainly suitable for analyzing branching ratios. While several studies have been devoted to fitting CP violation in $SU(3)$ flavour symmetry [112–116], the analysis of asymmetry parameters and CP violation in charmed baryon decays remains a major challenge. In addition, there are some analyses of charmed baryon decays based on dynamical models such as pole models, current algebra, and quark model [117–130]. However, these dynamical models usually have significant theoretical uncertainties, or are difficult to calculate the CP asymmetries of charmed baryon decays. Totally speaking, it is urgent to develop theoretical methods for describing the dynamics of charmed baryon decays and calculating its branching ratios, asymmetry parameters and CP violation.

Final-state interaction is a physical picture for the long-distance contributions of the weak decays of heavy-flavor hadrons. The observed CP violation of charmed meson decays in $D^0 \rightarrow K^+K^-$ and $\pi^+\pi^-$ indicates that the penguin diagrams are at the same order as the tree diagrams apart from the CKM matrix elements [131]. The enhancement of penguin diagrams might be induced by the long-distance contributions [132, 133]. The final-state-interaction effect can easily explain the similar size of penguin and tree diagrams, since they stem from the same hadronic triangle diagrams. For example, the final-state interactions have been used to explain the CP violation in D meson decays[134, 135], providing the results at the same order with the experimental observations. The rescattering mechanism, modeled as single-particle exchanges (one loop triangle diagrams), has been widely applied to calculate the final state interactions in heavy hadron non-leptonic decays, such as the systematic analysis on B meson two-body decays in [136] and the successful prediction on the discovery channels of doubly charmed baryon Ξ_{cc}^{++} in [137]. In the previous studies, the computation of the triangle diagrams in rescattering mechanism is based on the optical theorem and Cutkosky cutting rules, where only the imaginary parts of triangle amplitudes are involved and therefore difficult to describe the strong phases.

In this work, we improve the calculation method for the effects of final state interactions in the rescattering mechanism by utilizing the complete analytical expression of loop integrals and thus obtain the magnitude and strong phase of triangle diagrams. The weak transition vertices are obtained from the weak effective Hamiltonian using the naive factorization approach for the short-distance contributions, while the hadron strong scatterings are calculated using the hadronic effective Lagrangian for the long-distance contributions. We adopt the Pauli-Villars scheme with the momentum cutoff to regularize the divergence in the loop integrals, with a model dependent parameter corresponding to the cutoff. It can be demonstrated that the modification of the propagator in the Pauli-Villars scheme is consistent with the traditional approach of adding a monopole form factor to the propagator.

In our improved calculations, the explicit dependence of the branching fractions on the model

parameters is significantly reduced compared to conventional methods. As the $p\rho^0$ and $p\phi$ dominate the decays of $\Lambda_c^+ \rightarrow p\pi^+\pi^-$ and pK^+K^- , we study $\Lambda_c^+ \rightarrow \mathcal{B}_8 V$ decays in this work for CP violation, with \mathcal{B}_8 and V as octet baryons and vector mesons respectively. It is amazingly achieved that the results of branching ratios with only one model parameter, are consistent with all the nine existing experimental data of the $\Lambda_c^+ \rightarrow \mathcal{B}_8 V$ decays. Besides, we predict the CP violation of $\Lambda_c^+ \rightarrow \mathcal{B}_8 V$ decays for the first time, benefited from the non-trivial strong phases. It is also systematically studied for the decay asymmetry parameters in the angular distributions of final states. Since the decay asymmetry parameters and the CP asymmetry are defined as the ratios, the dependence of these observables on the model parameter and the input hadronic strong couplings is mostly cancelled in the ratios. The model dependence in the improved theoretical approach is therefore significantly reduced and is expected to provide a reasonable description of long-distance final state interactions.

We stress that the framework building up in this work can be naturally extended to the study of non-leptonic decays of charmed meson and bottom hadrons. For bottom hadron decays, although the factorizable contributions in perturbation theory may be important in magnitude, the effect of final state interactions is crucial for generating strong phases and thus for predicting CP violation.

In section II, we introduce the theoretical framework, including the topological diagrams for the classification of weak transitions, the naive factorization approach for calculating the short-distance contributions and the rescattering mechanism for estimating the long-distance final state interactions. In the third section, a discussion of the analytical expression of the three-point master integral will be involved, including the relation between the method of the complete loop integral and the Cutkosky cutting rule, proving the equivalence between the Pauli-Villars scheme with cutoff and the monopole form factors in the loop integral. We present the determination of input parameters and the obtained numerical results (the branching ratios, CP violation and decay asymmetry parameters for $\Lambda_c^+ \rightarrow \mathcal{B}_8 V$ decays) in section IV, where several channels, e.g. $\Lambda_c^+ \rightarrow p\rho^0$ and $\Lambda_c^+ \rightarrow p\phi$, are used to demonstrate the dependence of various observables on model and input parameters. A summary is given in the last section. Essential details regarding the amplitudes for all of the $\Lambda_c^+ \rightarrow \mathcal{B}_8 V$ channels are provided in Appendix A, while Appendix B contains expressions for the hadronic effective Lagrangian and the heavy to light form factors.

II. THEORETICAL FRAMEWORK

In this section, we firstly introduce the topological diagrams which are widely used to describe the heavy hadron non-leptonic decays[126, 138–141]. Then we demonstrate the general framework for calculating the short-distance and long-distance dynamics in each kind of topological diagram.

A. Topological diagrams and non-perturbative contribution

Topology diagrams contain perturbative and non-perturbative information in heavy baryon non-leptonic decays and provide an intuitive representation of the strong interaction dynamics in the weak decay. According to the diagram viewpoint, the tree-level topological diagrams for two-body non-leptonic weak decays of charmed baryons are listed in Fig.1. These diagrams are sorted by their different weak decay topologies[126]. T stands for the color-allowed diagram with the external W -emission, C and C' are both color-suppressed diagrams with internal W -emission, the difference between them is that the quark which is from the weak transition of charm quark flows into the final-state meson or baryon. Simialrly, there exist three different types of W -exchange diagrams which can be distinguished with the flow of quarks that generated from weak vertex and are respectively denoted as E_1 , E_2 and B .

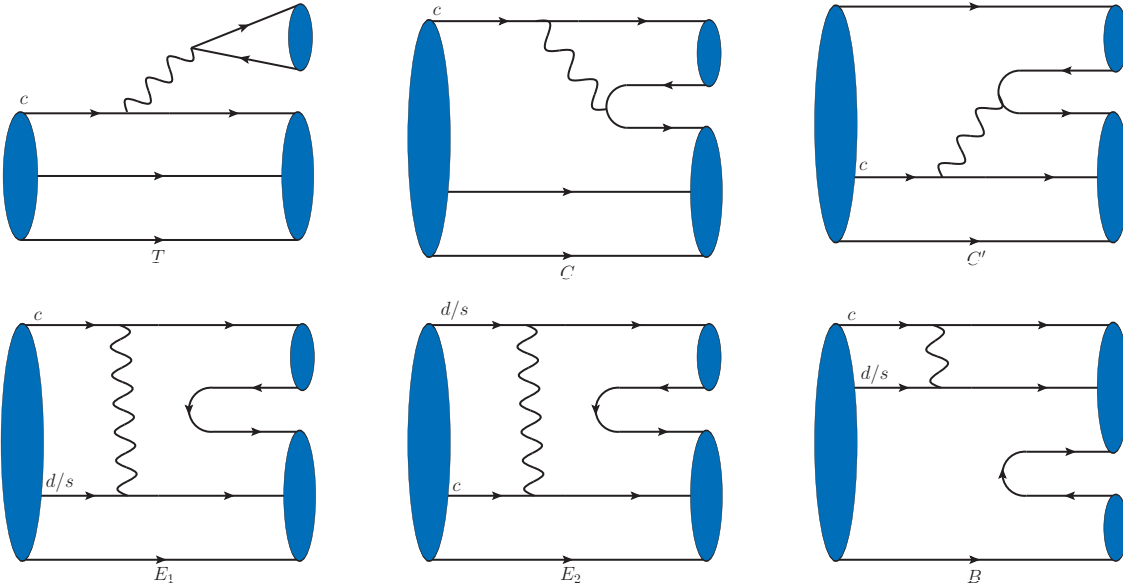


FIG. 1: Tree level topological diagrams for two-body nonleptonic decays of singly charmed baryon.

Generally, the topology diagrams involve factorization and non-factorization contributions. The T topology is dominated by factorizable contributions according to the color transparency mechanism and can be well estimated within the naive factorization approach, i.e., it can be expressed as the convolution of baryon weak transition form factors and meson's decay constants. For the internal W -emission diagram C , the short-distance contributions can also be calculated from the naive factorization approach, however which are suppressed by the small effective Wilson coefficients of four-fermion operators at charm scale[132, 142, 143]. Some studies have shown that the non-factorizable long-distance contributions of C are much more important than the short-distance contributions in heavy baryon decays[137, 144, 145]. Moreover, according to the power counting rules from the soft-collinear effective theory, the ratios among the topological diagrams have the following power counting relation, $\frac{|C|}{|T|} \sim \frac{|C'|}{|C|} \sim \frac{|E_1|}{|C|} \sim \frac{|E_2|}{|C|} \sim \frac{|B|}{|C|} \sim \mathcal{O}\left(\frac{\Lambda_{QCD}^h}{m_Q}\right)$ [146, 147], this factor is about $\mathcal{O}(1)$ at $m_c = 1.3\text{GeV}$. This means that the topology diagrams except for T are non-factorization contributions dominated and must be well-estimated in charm system.

To calculate the contributions of different topological diagrams in charmed baryon decays, we face challenges due to their non-perturbative nature. Direct computation of all the topological diagrams is impractical. Instead, we employ different theoretical methods to calculate the short and long-distance contributions of these topology diagrams. Typically, we use a naive factorization approach to estimate factorizable contributions. For non-factorizable contributions, such as final state interaction effects mediated by loop mechanisms, we incorporate these effects into our model. This approach allows us to refine theoretical predictions by adjusting parameters and assumptions, ensuring better agreement with experimental data.

B. Short-distance contributions with factorization hypothesis

In this part, we introduce the framework for estimating the short-distance factorizable contributions of the T and C diagram, which is the foundation for the calculation of the long-distance non-factorizable contributions based on the hypothesis of final-state rescattering

mechanism.

Firstly, we present the weak effective Hamiltonian which is generally used to analyse the non-leptonic decays of heavy hadrons,

$$\mathcal{H}_{eff} = \frac{G_F}{\sqrt{2}} \sum_{q'=d,s} V_{cq'}^* V_{uq} [C_1(\mu) O_1(\mu) + C_2(\mu) O_2(\mu)] + h.c. , \quad (1)$$

where $C_{1,2}(\mu)$ are Wilson coefficients including the short-distance QCD dynamics, $O_{1,2}(\mu)$ are the tree level four-fermion operators,

$$O_1 = (\bar{u}_\alpha q_\beta)_{V-A} (\bar{q}'_\beta c_\alpha)_{V-A}, \quad O_2 = (\bar{u}_\alpha q_\alpha)_{V-A} (\bar{q}'_\beta c_\beta)_{V-A}, \quad (2)$$

then, the hadronic matrix element of charmed baryon decay can be derived directly,

$$\langle \mathcal{B}_8 M | \mathcal{H}_{eff} | \mathcal{B}_c \rangle = \frac{G_F}{\sqrt{2}} V_{cq'}^* V_{uq} \sum_{i=1,2} C_i \langle \mathcal{B}_8 M | O_i | \mathcal{B}_c \rangle , \quad (3)$$

here, we neglect the contributions of penguin operators due to the large suppression of CKM matrix element in charmed hadron decays.

A further step is to deal with the hadronic matrix element of four-fermion operators $\langle \mathcal{B}_8 M | O_i | \mathcal{B}_c \rangle$. The well known approach is the naive factorization governed by the color transparency mechanism, the hadronic matrix element is factorized as the convolution of two parts

$$\langle \mathcal{B}_8 M | O_i | \mathcal{B}_c \rangle \rightarrow \langle M | \mathcal{J}_{uq}^\mu | 0 \rangle \otimes \langle \mathcal{B}_8 | \mathcal{J}_{\mu,cq'} | \mathcal{B}_c \rangle , \quad (4)$$

where \mathcal{J}_{uq}^μ and $\mathcal{J}_{\mu,cq'}$ represent the $V - A$ current with the quark flavor (uq) and $(q'c)$ respectively. The proof for this factorization can be extended from the studies of bottom hadron decays, as discussed in references [2–5]. Based on the factorization formula, the T and C topology are given by

$$\langle \mathcal{B}_8 M | \mathcal{H}_{eff} | \mathcal{B}_c \rangle_{SD}^T = \frac{G_F}{\sqrt{2}} V_{cq'}^* V_{uq} a_1(\mu) \langle M | \bar{u} \gamma^\mu (1 - \gamma_5) q | 0 \rangle \langle \mathcal{B}_8 | \bar{q}' \gamma_\mu (1 - \gamma_5) c | \mathcal{B}_c \rangle , \quad (5a)$$

$$\langle \mathcal{B}_8 M | \mathcal{H}_{eff} | \mathcal{B}_c \rangle_{SD}^C = \frac{G_F}{\sqrt{2}} V_{cq'}^* V_{uq} a_2(\mu) \langle M | \bar{u} \gamma^\mu (1 - \gamma_5) q | 0 \rangle \langle \mathcal{B}_8 | \bar{q}' \gamma_\mu (1 - \gamma_5) c | \mathcal{B}_c \rangle , \quad (5b)$$

where $a_{1,2}(\mu)$ are the effective Wilson coefficients defined through $a_1(\mu) = C_1(\mu) + C_2(\mu)/3$, $a_2(\mu) = C_2(\mu) + C_1(\mu)/3$ with $C_1(\mu) = 1.21$, $C_2(\mu) = -0.42$ evolved from M_W to the charm scale $\mu = m_c$ [132]. In Eq.(5a) and (5b), the first matrix element $\langle M | \mathcal{J}_{uq}^\mu | 0 \rangle$ is parameterized as the meson's decay constants [148]

$$\langle P(p) | \bar{u} \gamma^\mu (1 - \gamma_5) q | 0 \rangle = i f_P p^\mu , \quad (6a)$$

$$\langle V(p) | \bar{u} \gamma^\mu (1 - \gamma_5) q | 0 \rangle = m_V f_V \varepsilon^{*\mu} , \quad (6b)$$

where $f_{P,V}$ are the decay constant of pseudoscalar and vector mesons respectively, and ε^μ is the polarization vector. The second one $\langle \mathcal{B}_8 | \mathcal{J}_{\mu,cq'} | \mathcal{B}_c \rangle$ is formulated as the heavy-to-light transition form factors

$$\begin{aligned} \langle \mathcal{B}_8(p_f, s_f) | \bar{q}' \gamma_\mu (1 - \gamma_5) c | \mathcal{B}_c(p_i, s_i) \rangle &= \bar{u}(p_f, s_f) \left[\gamma_\mu f_1(q^2) + i \sigma_{\mu\nu} \frac{q^\nu}{m_i} f_2(q^2) + \frac{q^\mu}{m_i} f_3(q^2) \right] u(p_i, s_i) \\ &\quad - \bar{u}(p_f, s_f) \left[\gamma_\mu g_1(q^2) + i \sigma_{\mu\nu} \frac{q^\nu}{m_i} g_2(q^2) + \frac{q^\mu}{m_i} g_3(q^2) \right] \gamma_5 u(p_i, s_i) , \end{aligned} \quad (7)$$

with momentum transfer $q = p_i - p_f$, f_i and g_i are heavy-to-light transition form factors which can be calculated through non-perturbative approaches. Conventionally, the amplitude of two-body non-leptonic charmed baryon decays is given in terms of partial wave scheme

$$\mathcal{A}(\mathcal{B}_c \rightarrow \mathcal{B}_8 P) = i\bar{u}_f(A + B\gamma_5)u_i, \quad (8)$$

specifically, the invariant amplitudes A and B are expressed as the following factorization form by using the form factor f_i and g_i

$$A = \lambda f_P(m_i - m_f)f_1(m^2), \quad B = \lambda f_P(m_i + m_f)g_1(m^2). \quad (9)$$

For vector meson, the amplitudes are

$$\mathcal{A}(\mathcal{B}_c \rightarrow \mathcal{B}_8 V) = \bar{u}_f \left(A_1 \gamma_\mu \gamma_5 + A_2 \frac{p_{f\mu}}{m_i} \gamma_5 + B_1 \gamma_\mu + B_2 \frac{p_{f\mu}}{m_i} \right) \varepsilon^{*\mu} u_i, \quad (10)$$

where

$$A_1 = -\lambda f_V m \left(g_1(m^2) + g_2(m^2) \frac{m_i - m_f}{m_i} \right), \quad A_2 = -2\lambda f_V m g_2(m^2), \quad (11)$$

$$B_1 = \lambda f_V m \left(f_1(m^2) - f_2(m^2) \frac{m_i + m_f}{m_i} \right), \quad B_2 = 2\lambda f_V m f_2(m^2), \quad (12)$$

with $\lambda = \frac{G_F}{\sqrt{2}} V_{cq'}^* V_{uq} a_{1,2}(\mu)$ for simplicity, m is the mass of final meson. As we mentioned before, the factorization formula in Eq.(8) and (10) are also essential ingredients for calculating the long-distance final-state interaction effects. And the decay width has the form with partial-wave amplitudes,

$$\Gamma(\mathcal{B}_c \rightarrow \mathcal{B}_8 V) = \frac{p_c(E_f + m_f)}{4\pi m_i} \left[2(|S|^2 + |P_2^2|) + \frac{E_V^2}{m_V^2} (|S + D|^2 + |P_1|^2) \right], \quad (13)$$

with the relations as following,

$$\begin{aligned} S &= -A_1, \\ P_1 &= -\frac{p_c}{E_V} \left(\frac{m_i + m_f}{E_f + m_f} B_1 + B_2 \right), \\ P_2 &= \frac{p_c}{E_f + m_f} B_1, \\ D &= -\frac{p_c^2}{E_V(E_f + m_f)} (A_1 - A_2). \end{aligned} \quad (14)$$

C. Long-distance contributions with final-state rescattering mechanism

In this section, we concentrate on the calculation of the long-distance contributions for the topology C, C', E_1, E_2 and B . The long-distance contributions are considerably important in charmed baryon decays, but it is notoriously difficult to study final-state interaction effects (FSIs) in a systematical way as it is non-perturbative in nature.

The final-state rescatterings provide a natural physical picture for the long-distance contributions of the heavy hadron decays. Wolfenstein and Sukuzi proposed the formalism of final-state interaction at the hadronic level based on CPT invariance and unitarity [149, 150]. Cheng, Chua and Soni performed a comprehensive study on B -meson two-body decays considering

FSI effects [136]. Using a time evolution picture [151], the short-distance interactions happen rapidly and violently at the beginning of weak decays, while the long-distance interactions happen at a much later time. The full amplitude is expressed as [151]

$$\mathcal{A} = \mathcal{S}^{1/2} \mathcal{A}_0, \quad (15)$$

where \mathcal{A}_0 is free from any strong phase, and the S -matrix $\mathcal{S}^{1/2}$ is a time-evolution operator $U(\infty, 0)$. In the picture of final-state rescattering, the above formula could be expressed as $\mathcal{A}_i = \sum_j \mathcal{S}_{ij}^{1/2} \mathcal{A}_{0j}$. At a short time after the weak interaction, the quarks and gluons are good degrees of freedom, so that \mathcal{A}_{0j} corresponds to the factorizable contributions given in the above subsection whose strong phase is vanishing. Then the states j are rescattered into the final states i via $\mathcal{S}_{ij}^{1/2}$ which usually contribute the non-zero strong phases. The derivation and detailed explanations are referred to [150–152]. It has been manifested that the final-state rescatterings are very important in the CP violation of three-body B meson decays[150, 153–155] and also in the CPV of charmed meson decays[134, 135, 156].

Following the previous studies in [136, 157], we can gain some control on re-scattering effects by studying them in a phenomenological way, that is the FSIs can be treated approximately as the one-particle-exchange processes at the hadron level. Under this mechanism, the charmed baryon two-body decays are described by triangle or bubble diagrams, the weak transitions are followed by the hadronic particle exchange/annihilation process. The triangle diagrams for the description of FSIs in charmed baryon decays are listed in Fig.2. It has been argued that the two-body scatterings dominate the FSIs, while the three-body and four-body intermediate states are negligible or relatively small [158, 159] and we assume that two-body to n-body scatterings are negligible due to the limited phase space. We only consider the $2 \rightarrow 2$ scattering processes in present calculation.

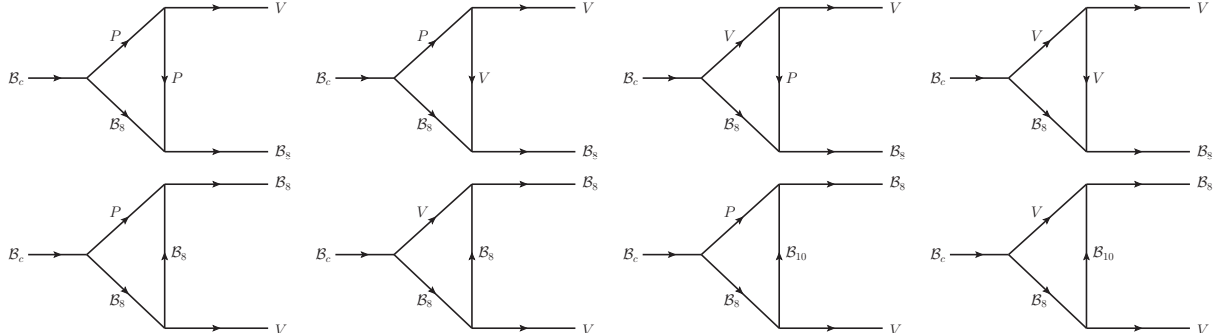


FIG. 2: The long-distance re-scattering contributions to $\Lambda_c^+ \rightarrow \mathcal{B}_8 V$ at hadron level.

In order to calculate the diagrams in Fig.2, we need to combine the formula of the weak transition vertex (described by the weak effective Hamiltonian and naive factorization) and the hadronic scattering amplitudes (governed by the effective hadronic Lagrangian which are collected in the App.B). To avoid double counting, the two-body weak transition amplitudes of charmed baryon only involve the short-distance factorizable contributions which we have introduced in last section. For estimating the hadronic scattering amplitudes, we need the following Feynman rules derived

from the matrix element of the effective hadronic Lagrangian with definite initial and final states,

$$\langle V(k, \lambda_k) P(p_2) | i\mathcal{L}_{VPP} | P(p_1) \rangle = -ig_{VVP} \varepsilon^{*\mu}(k, \lambda_k) (p_1 + p_2)_\mu, \quad (16)$$

$$\langle \mathcal{B}_2(p_2) P(q) | i\mathcal{L}_{PBB} | \mathcal{B}_1(p_1) \rangle = g_{BBP} \bar{u}(p_2) i\gamma_5 u(p_1), \quad (17)$$

$$\langle \mathcal{B}_2(p_2) V(q, \lambda_q) | i\mathcal{L}_{VBB} | \mathcal{B}_1(p_1) \rangle = \bar{u}(p_2) \left[f_1 \gamma_\nu + f_2 \frac{i}{m_1 + m_2} \sigma_{\mu\nu} q^\mu \right] \varepsilon^{*\nu}(q, \lambda_q) u(p_1), \quad (18)$$

$$\langle V(p_3, \lambda_3) V(k, \lambda_k) | i\mathcal{L}_{VVP} | P(p_1) \rangle = -i \frac{g_{VVP}}{f_p} \epsilon^{\mu\nu\alpha\beta} p_3 \mu \varepsilon_\nu^*(\lambda_3, p_3) k_\alpha \varepsilon_\beta^*(k, \lambda_k), \quad (19)$$

$$\begin{aligned} \langle B(p_4, \lambda_4) | i\mathcal{L}_{VBD} | D(k, \lambda_k) V(p_1, \lambda_1) \rangle &= -i \frac{g_{\rho N \Delta}}{m_\rho} \bar{u}(p_4, \lambda_4) \gamma^5 \gamma^\nu u^\mu(k, \lambda_k) \\ &\times [p_1 \mu \varepsilon_\nu(p_1, \lambda_1) - p_1 \nu \varepsilon_\mu(p_1, \lambda_1)], \end{aligned} \quad (20)$$

$$\langle B(p_4, \lambda_4) | i\mathcal{L}_{VBD} | D(k, \lambda_k) P(p_1, \lambda_1) \rangle = \frac{g_{\pi N \Delta}}{m_\pi} \bar{u}(p_4, \lambda_4) p_1 \mu u^\mu(k, \lambda_k), \quad (21)$$

$$\begin{aligned} \langle V(p_3, \lambda_3) V(k, \lambda_k) | i\mathcal{L}_{VVV} | V(p_1, \lambda_1) \rangle &= -\frac{ig_{VVV}}{\sqrt{2}} \varepsilon_\mu(p_1, \lambda_1) \varepsilon^{\mu*}(p_3, \lambda_3) \varepsilon_\nu^*(k, \lambda_k) (p_3^\nu + p_1^\nu) \\ &- \frac{ig_{VVV}}{\sqrt{2}} \varepsilon_\mu^*(k, \lambda_k) \varepsilon^\mu(p_1, \lambda_1) \varepsilon_\nu^*(p_3, \lambda_3) (-p_1^\nu - p_k^\nu) \\ &- \frac{ig_{VVV}}{\sqrt{2}} \varepsilon_\mu^*(p_3, \lambda_3) \varepsilon^{*\mu}(k, \lambda_k) \varepsilon_\nu(p_1, \lambda_1) (p_k^\nu - p_3^\nu). \end{aligned} \quad (22)$$

Then, we arrive at the analytical expression of the eight hardonic loop diagrams by applying the factorization formula of the weak transition amplitudes and the above Feynman rules of the hadronic couplings. For simplicity, we unify the symbols of momentum and spin polarization through following rule $\Lambda_c^+(p_i, s_i) \rightarrow \mathcal{B}_8(p_3, s_3)V(p_4, \epsilon_4)$ with re-scattering particle $\mathcal{B}_8(p_1, s_1)P(p_2)/V(p_2, \epsilon_2)$ and exchanged one $P(k), V(k, \varepsilon_k), B/D(k, s_k)$. Under this convention, we obtain the amplitudes of the eight triangle diagrams with the loop integral variable k ,

$$\begin{aligned} \mathcal{M}[P, \mathcal{B}_8; P] &= -i \int \frac{d^4 k}{(2\pi)^4} g_{BBP} \cdot g_{VPP} \bar{u}(p_4, s_4) \gamma_5 (\not{p}_2 + m_2) (A + B \gamma_5) u(p, s) \\ &\times \varepsilon_\mu^*(p_3, \lambda_3) (p_1 + k)^\mu \frac{\mathcal{F}}{(p_1^2 - m_1^2 + i\epsilon)(p_2^2 - m_2^2 + i\epsilon)(k^2 - m_k^2 + i\epsilon)}, \end{aligned} \quad (23)$$

$$\begin{aligned} \mathcal{M}[P, \mathcal{B}_8; V] &= - \int \frac{d^4 k}{(2\pi)^4} \frac{4g_{VVP}}{f_P} \bar{u}(p_4, s_4) \left[f_{1BBV} \gamma_\delta - \frac{if_{2BBV}}{m_2 + m_4} \sigma_{\sigma\delta} k^\sigma \right] \\ &\times (A + B \gamma_5) u(p, s) \epsilon_{\mu\nu\alpha\delta} p_3^\mu \varepsilon^{*\nu}(p_3, \lambda_3) k^\alpha (\not{p}_2 + m_2) \\ &\times \frac{\mathcal{F}}{(p_1^2 - m_1^2 + i\epsilon)(p_2^2 - m_2^2 + i\epsilon)(k^2 - m_k^2 + i\epsilon)}, \end{aligned} \quad (24)$$

$$\begin{aligned} \mathcal{M}[V, \mathcal{B}_8; P] &= i \int \frac{d^4 k}{(2\pi)^4} \frac{4g_{VVP}}{f_p} g_{BBP} \bar{u}(p_4, s_4) \gamma_5 (\not{p}_2 + m_2) \\ &\times \left(A_1 \gamma_\delta \gamma_5 + A_2 \frac{p_{2\delta}}{m_i} \gamma_5 + B_1 \gamma_\delta + B_2 \frac{p_{2\delta}}{m_i} \right) \epsilon_{\mu\nu\alpha\delta} p_3^\mu \varepsilon^{*\nu}(p_3, \lambda_3) p_1^\alpha u(p, s) \\ &\times \frac{\mathcal{F}}{(p_1^2 - m_1^2 + i\epsilon)(p_2^2 - m_2^2 + i\epsilon)(k^2 - m_k^2 + i\epsilon)}, \end{aligned} \quad (25)$$

$$\begin{aligned}
\mathcal{M}[V, \mathcal{B}_8; V] = & -i \int \frac{d^4 k}{(2\pi)^4} \bar{u}(p_4, s_4) (f_{1BBV} \gamma_\delta - \frac{i f_{2BBV}}{m_2 + m_4} \sigma_{\sigma\delta} k^\sigma) (\not{p}_2 + m_2) \\
& \times \left(A_1 \gamma^\alpha \gamma_5 + A_2 \frac{p_2^\alpha}{m_i} \gamma_5 + B_1 \gamma^\alpha + B_2 \frac{p_2^\alpha}{m_i} \right) u(p, s) \\
& \times g_{VVV} \left[\left(-g^{\delta\mu} + \frac{k^\delta k^\mu}{m_k^2} \right) \left(-g_{\mu\alpha} + \frac{p_{1\mu} p_{1\alpha}}{m_1^2} \right) \varepsilon_\nu^*(p_3, \lambda_3) (k + p_1)^\nu \right. \\
& + \varepsilon_\mu^*(p_3, \lambda_3) \left(-g^{\delta\mu} + \frac{k^\delta k^\mu}{m_k^2} \right) \left(-g_{\nu\alpha} + \frac{p_{1\nu} p_{1\alpha}}{m_1^2} \right) (p_3 - k)^\nu \\
& \left. + \left(-g_{\mu\alpha} + \frac{p_{1\mu} p_{1\alpha}}{m_1^2} \right) \varepsilon^{\mu*}(p_3, \lambda_3) \left(-g^{\delta\nu} + \frac{k^\delta k^\nu}{m_k^2} \right) (-p_1 - p_3)_\nu \right] \\
& \times \frac{\mathcal{F}}{(p_1^2 - m_1^2 + i\epsilon)(p_2^2 - m_2^2 + i\epsilon)(k^2 - m_k^2 + i\epsilon)}, \tag{26}
\end{aligned}$$

$$\begin{aligned}
\mathcal{M}[P, \mathcal{B}_8; \mathcal{B}_8] = & -i \int \frac{d^4 k}{(2\pi)^4} g_{BBP} \bar{u}(p_4, s_4) \gamma_5 (\not{k} + m_k) \left[f_{1BBV} \gamma_\nu + \frac{i f_{2BBV}}{m_2 + m_k} \sigma_{\mu\nu} p_3^\mu \right] \\
& \times \varepsilon^{\nu*}(p_3, \lambda_3) (\not{p}_2 + m_2) (A + B \gamma_5) u(p, s) \\
& \times \frac{\mathcal{F}}{(p_1^2 - m_1^2 + i\epsilon)(p_2^2 - m_2^2 + i\epsilon)(k^2 - m_k^2 + i\epsilon)}, \tag{27}
\end{aligned}$$

$$\begin{aligned}
\mathcal{M}[V, \mathcal{B}_8; \mathcal{B}_8] = & i \int \frac{d^4 p_1}{(2\pi)^4} \bar{u}(p_4, s_4) \left[f_{11BBV} \gamma_\delta - \frac{i f_{12BBV}}{m_4 + m_k} \sigma_{\sigma\delta} p_1^\sigma \right] (\not{k} + m_k) \\
& \times \left[f_{21BBV} \gamma_\nu + \frac{i f_{22BBV}}{m_2 + m_k} \sigma_{\mu\nu} p_3^\mu \right] \left(-g^{\delta\alpha} + \frac{p_1^\delta p_1^\alpha}{m_1^2} \right) \\
& \times \varepsilon^{*\nu}(p_3, \lambda_3) (\not{p}_2 + m_2) (A_1 \gamma_\alpha \gamma_5 + A_2 \frac{p_{2\alpha}}{m_i} \gamma_5 + B_1 \gamma_\alpha + B_2 \frac{p_{2\alpha}}{m_i}) u(p, s) \\
& \times \frac{\mathcal{F}}{(p_1^2 - m_1^2 + i\epsilon)(p_2^2 - m_2^2 + i\epsilon)(k^2 - m_k^2 + i\epsilon)}, \tag{28}
\end{aligned}$$

$$\begin{aligned}
\mathcal{M}[P, \mathcal{B}_8, \mathcal{B}_{10}] = & i \frac{g_{\rho\Delta N} g_{\pi\Delta N}}{m_\rho m_\pi} \int \frac{d^4 k}{(2\pi)^4} \bar{u}(p_4, \lambda_4) p_{1,\mu} P^{\mu\alpha} \gamma^5 \gamma^\beta (\not{p}_2 + m_2) \\
& \times [p_{3\alpha} \varepsilon_\beta^*(p_3, \lambda_3) - p_{3\beta} \varepsilon_\alpha^*(p_3, \lambda_3)] [A + B \gamma_5] u(p_i, \lambda_i) \\
& \times \frac{\mathcal{F}}{(p_1^2 - m_1^2 + i\epsilon)(p_2^2 - m_2^2 + i\epsilon)(k^2 - m_k^2 + i\epsilon)}, \tag{29}
\end{aligned}$$

$$\begin{aligned}
\mathcal{M}[V, \mathcal{B}_8, \mathcal{B}_{10}] = & \frac{g_{\rho\Delta N 1} g_{\rho\Delta N 2}}{m_{\rho 1} m_{\rho 2}} \int \frac{d^4 k}{(2\pi)^4} \bar{u}(p_4, \lambda_4) \gamma^5 \gamma^\nu P^{\mu\beta} \gamma^5 \gamma^\sigma (\not{p}_2 + m_2) \\
& \times \left[A_1 \gamma_\alpha \gamma_5 + A_2 \frac{p_{2\alpha}}{m_i} \gamma_5 + B_1 \gamma_\alpha + B_2 \frac{p_{2\alpha}}{m_i} \right] (-g_{\alpha\nu} p_{1\mu} + g_{\alpha\mu} p_{1\nu}) \\
& \times (p_{3\beta} \varepsilon_\sigma^*(p_3, \lambda_3) - p_{3\sigma} \varepsilon_\beta^*(p_3, \lambda_3)) \\
& \times \frac{\mathcal{F}}{(p_1^2 - m_1^2 + i\epsilon)(p_2^2 - m_2^2 + i\epsilon)(k^2 - m_k^2 + i\epsilon)}, \tag{30}
\end{aligned}$$

where $P^{\mu\alpha}$ denotes $\sum_s u_\mu(p, s) \bar{u}_\alpha(p, s)$ and the monopole form factor

$$\mathcal{F} = \left(\frac{\Lambda_1^2 - m_1^2}{\Lambda_1^2 - p_1^2} \right) \left(\frac{\Lambda_2^2 - m_2^2}{\Lambda_2^2 - p_2^2} \right), \tag{31}$$

is to regulate the possible divergence in the loop integrals. For completing the calculation, we need

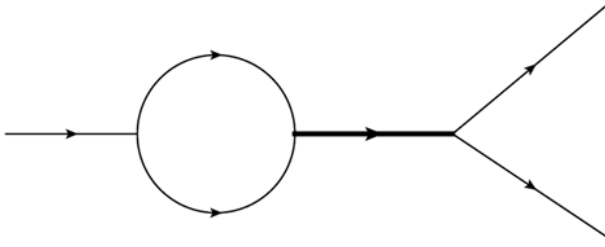


FIG. 3: Final state interaction effects with s -channel.

the following spin summation formula

$$\sum_s u(p, s) \bar{u}(p, s) = \not{p} + m, \quad (32)$$

$$\sum_s u_\mu(p, s) \bar{u}_\nu(p, s) = (\not{p} + m) \left\{ -g_{\mu\nu} + \frac{\gamma_\mu \gamma_\nu}{3} + \frac{2p_\mu p_\nu}{3m^2} - \frac{p_\mu \gamma_\nu - p_\nu \gamma_\mu}{3m} \right\}, \quad (33)$$

for $\frac{1}{2}$ and $\frac{3}{2}$ spinor respectively and the polarization summation of massive vector meson

$$\sum_{\lambda_1} \varepsilon^{*\rho}(p_1, \lambda_1) \varepsilon^\nu(p_1, \lambda_1) = -g^{\rho\nu} + \frac{p_1^\rho p_1^\nu}{m_1^2}. \quad (34)$$

In principle, the sum over all allowed intermediate two-body states is required by the unitarity and completeness of theory. However, as aforementioned, the contributions of multi-body states and much higher excited states in the intermediate state are suppressed due to the constraints of phase space.

In addition, it is also difficult to calculate the contributions from all orders. Therefore, in practical applications, we focus on the most important contributions of the intermediate processes and include as many computable contributions as possible in order to more accurately describe the impact of the intermediate states.

It should be noted that the final-state interactions not only involve the above-mentioned t/u channel single-particle exchange contributions, but also have the s channel contributions from resonance states which is formed as the bubble diagram in Fig.3. For b -hadron decays, the contributions from s channel can be neglected safely, the reason is that the mass of b -hadron is above 5GeV, and the light hadrons and charmed hadrons produced in this decay do not have such high excited states. In charm decays, there are several light hadron excited states at the energy region of charmed hadron. However, the excited states have large width in general, and the width effects of high excited states in propagator can not be neglected,

$$S \sim \frac{1}{p^2 - m^2 + im\Gamma}, \quad (35)$$

hence, the contribution of s -channel for charmed hadron decay will be suppressed by width effects of resonance states.

In essence, incorporating all conceivable intermediate states into final state interaction calculations proves unfeasible. The reliability of strong coupling inputs diminishes notably for higher excited states, resulting in increased uncertainties. Even if these states contribute, excessive uncertainty undermines the validity of our calculations. Therefore, our focus remains on S -wave states exclusively, currently disregarding s -channel contributions. This means our analysis includes only pseudoscalar and vector mesons, along with octet and decuplet baryons in triangle diagrams.

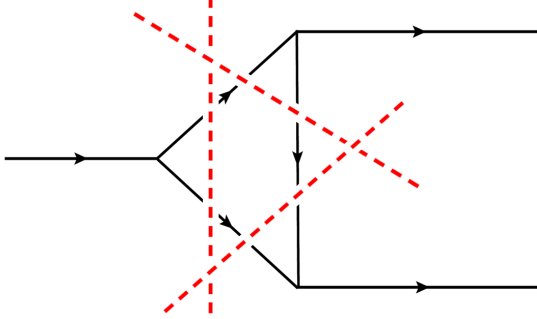


FIG. 4: The Cutkosky cutting rules of three-point master integrals.

III. ANALYTICAL DISCUSSIONS

A. Cutkosky cutting rule and Feynman loop integral

In the traditional approach [136], the amplitude of the triangle diagram is usually calculated by utilizing optical theorem and Cutkosky cutting rule to obtain the imaginary part. The real part of the triangle diagram can be derived from the dispersion relation in principle, but due to the large ambiguity, the amplitude in the whole region cannot be reliably described, so this effect is ignored in many works. Therefore, the traditional method is not thorough in calculating the triangle diagram and therefore loses the information

In order to obtain the complete amplitude of the triangle diagram, the most natural approach is to calculate the loop integrals. In this work, we adopt the Passarino-Veltman (PV) method to reduce the tensor integrals and the method of integral by parts (IBP) to obtain the expressions with master integrals. Then we obtain the numerical results for the master integrals by means of Looptools. In the following, we present the proof that the imaginary part of a general three-point master integral (displayed in Fig.4) which is directly calculated from the analytical expression is consistent with the one by summing over all of cutting ways which is required by Cutkosky cutting rule. For simplicity, we adopt the convention $p^2 = (p_3 + p_4)^2 = m_i^2$, $p_3^2 = p_4^2 = m_f^2$, $m_1^2 = m_2^2 = m_k^2 = m_1^2$. The imaginary part of the three-point master integral is obtained from the directly computed analytical expression by integrating out the loop-momentum k ,

$$\begin{aligned}
& \text{Im}(-i) \int \frac{d^4 k}{(2\pi)^4} \frac{1}{k^2 - m_1^2 + i\varepsilon} \frac{1}{(k - p_1)^2 - m_1^2 + i\varepsilon} \frac{1}{(k - p_1 - p_2)^2 - m_1^2 + i\varepsilon} \\
&= -\frac{1}{16\pi^2} \text{Im} \int_0^1 dx \int_0^{1-x} \frac{dy}{m_i^2 x^2 + m_f^2 y^2 + m_i^2 x y - m_i^2 x - m_f^2 y + m_1^2 - i\varepsilon} \\
&= -\frac{1}{16\pi} \int_0^1 dx \int_0^{1-x} dy \delta(m_i^2 x^2 + m_f^2 y^2 + m_i^2 x y - m_i^2 x - m_f^2 y + m_1^2) \\
&= \begin{cases} \frac{1}{16\pi m_i \sqrt{(m_i^2 - 4m_f^2)}} \ln \left[\frac{m_i^2 - 2m_f^2 - \sqrt{(m_i^2 - 4m_f^2)(m_i^2 - 4m_1^2)}}{m_i^2 - 2m_f^2 + \sqrt{(m_i^2 - 4m_f^2)(m_i^2 - 4m_1^2)}} \left(\frac{m_i m_f + \sqrt{(m_i^2 - 4m_f^2)(m_f^2 - 4m_1^2)}}{m_i m_f - \sqrt{(m_i^2 - 4m_f^2)(m_f^2 - 4m_1^2)}} \right)^2 \right] & \forall m_1 \in (0, \frac{m_f}{2}), \\ \frac{1}{16\pi m_i \sqrt{m_i^2 - 4m_f^2}} \ln \frac{m_i^2 - 2m_f^2 - \sqrt{(m_i^2 - 4m_f^2)(m_i^2 - 4m_1^2)}}{m_i^2 - 2m_f^2 + \sqrt{(m_i^2 - 4m_f^2)(m_i^2 - 4m_1^2)}} & \forall m_1 \in (\frac{m_f}{2}, \frac{m_i}{2}), \\ 0 & \forall m_1 \in (\frac{m_i}{2}, \infty), \end{cases} \quad (36)
\end{aligned}$$

and the one calculated from the Cutkosky cutting rule is,

$$\begin{aligned}
& \text{Im}(-i) \int \frac{d^4 k}{(2\pi)^4} \frac{1}{k^2 - m_1^2 + i\varepsilon} \frac{1}{(k - p_1)^2 - m_1^2 + i\varepsilon} \frac{1}{(k - p_1 - p_2)^2 - m_1^2 + i\varepsilon} \\
&= P \int \frac{d^4 k}{8\pi^2} \left[\frac{\theta[k_0] \delta(k^2 - m_1^2) \theta[p_{10} + p_{20} - k_0] \delta((p_1 + p_2 - k)^2 - m_1^2)}{(k - p_1)^2 - m_1^2 + i\varepsilon} \right. \\
&\quad + \frac{\theta[k_0] \delta(k^2 - m_1^2) \theta[p_{10} - k_0] \delta((p_1 - k)^2 - m_1^2)}{(k - p_1 - p_2)^2 - m_1^2 + i\varepsilon} \\
&\quad \left. + \frac{\theta[k_0 - p_{10}] \delta((k - p_1)^2 - m_1^2) \theta[p_{10} + p_{20} - k_0] \delta((p_1 + p_2 - k)^2 - m_1^2)}{k^2 - m_1^2 + i\varepsilon} \right] \\
&= \frac{\theta[m_i - 2m_1]}{16\pi m_i \sqrt{m_i^2 - 4m_f^2}} \ln \left| \frac{m_i^2 - 2m_f^2 - \sqrt{(m_i^2 - 4m_f^2)(m_i^2 - 4m_1^2)}}{m_i^2 - 2m_f^2 + \sqrt{(m_i^2 - 4m_f^2)(m_i^2 - 4m_1^2)}} \right| \\
&\quad + \frac{\theta[m_f - 2m_1]}{8\pi m_i \sqrt{m_i^2 - 4m_f^2}} \ln \left| \frac{m_i m_f + \sqrt{(m_i^2 - 4m_f^2)(m_f^2 - 4m_1^2)}}{m_i m_f - \sqrt{(m_i^2 - 4m_f^2)(m_f^2 - 4m_1^2)}} \right|. \tag{37}
\end{aligned}$$

based on the properties of the Theta function, it is clear that the results in first line of Eq.(37) satisfy the range $m_1 \in (0, \frac{m_i}{2})$, it includes both the region $m_1 \in (0, \frac{m_f}{2})$ and the region $m_1 \in (\frac{m_f}{2}, \frac{m_i}{2})$, and the results in second line only satisfy the range $m_1 \in (0, \frac{m_f}{2})$. Then, it is not difficult to transform the results in Eq.(37) into the results in Eq.(36). Hence, we can demonstrate the results in Eq.(36) and Eq.(37) are consistent with each other. The corresponding proof can be extended to the case of any other one-loop master integrals and even higher-loop diagrams [160, 161].

B. Pauli-Villars regularization and model form factors

In our calculation, the hadronic couplings are essential inputs and usually are estimated with the initial and final hadron states on-shell. In the triangle diagram, the hadronic couplings need to be modified with the effects that the internal particles have off-shell momentum. This is the first reason to introduce the form factor parameterized as follows,

$$\mathcal{F} = \left(\frac{m^2 \pm \Lambda^2}{p^2 \pm \Lambda^2} \right)^n, \quad \Lambda = m + \eta \Lambda_{QCD}, \tag{38}$$

where the signs “+ / -” are corresponding to the s-channel and t/u-channel respectively, m and p are the mass and momentum of propagator and $\Lambda_{QCD} = 330\text{MeV}$ is the nonperturbative scale in charm quark decay. It has been argued that the monopole behavior of the form factor with $n = 1$ is much more consistent with the results that expected by the QCD sum rule [162].

The second reason is that we need to introduce an appropriate regularization scheme to regulate the inevitable divergence appearing in the master integrals of the triangle diagram amplitude. The introduced form factor in Eq.(38) is consistent with the Pauli-Villars regularization scheme. We present some details for deriving the form factor from the Pauli-Villars scheme in the following. The idea is to introduce a heavy particle that coupled to the propagator, that is the propagator can be rewritten as,

$$\begin{aligned}
\frac{1}{k^2 - m^2 + i\epsilon} &\Rightarrow \frac{1}{k^2 - m^2 + i\epsilon} + \frac{a_1}{k^2 - \Lambda_1^2 + i\epsilon} \\
&\Rightarrow \frac{k^2 - \Lambda_1^2 + a_1(k^2 - m^2)}{(k^2 - m^2)(k^2 - \Lambda_1^2)}, \tag{39}
\end{aligned}$$

TABLE I: The decay constants of pseudoscalar [163] and vector [164] mesons.

Decay constant	f_π	f_K	f_ρ	f_ω	f_ϕ	f_{K^*}
Value [MeV]	130.2 ± 0.12	155.7 ± 0.3	216 ± 3	187 ± 5	215 ± 5	220 ± 5

where $\Lambda_1 \gg m^2$ is the cutoff scale, a_1 is an undetermined coefficient. When we take the value of a_1 is equal to -1 , the superficial degree of divergence of the integral is obviously reduced and the expression in Eq.(39) can be simplified as,

$$\frac{1}{k^2 - m^2 + i\epsilon} \rightarrow \frac{m^2 - \Lambda_1^2}{(k^2 - m^2)(k^2 - \Lambda_1^2)} = \frac{1}{k^2 - m^2} \frac{m^2 - \Lambda_1^2}{k^2 - \Lambda_1^2}, \quad (40)$$

where the factor $(m^2 - \Lambda_1^2)/(k^2 - \Lambda_1^2)$ is nothing but the monopole form factor we introduced in Eq.(38). If we encounter integrals with higher divergences, we can address this by introducing couplings with heavier particles. However, we won't delve into this approach here. The cutoff scale Λ is chosen to follow the same parameterized form as in the conventional method [136],

$$\Lambda = m + \eta \Lambda_{QCD}, \quad (41)$$

where m represents the mass of the propagator, the only parameter is η , which can be determined from experimental data.

IV. NUMERICAL RESULTS AND DISCUSSION

In this section, we present the determination of the various input parameters and the numerical results for the branching ratios, decay asymmetry parameters and CP violations of the $\Lambda_c \rightarrow \mathcal{B}_8 V$ channels.

A. Inputs

We take the hadron masses and the decay constants of pseudoscalar mesons from the Particle Data Group [163]. The decay constants of vector mesons are obtained from the comprehensive analysis in [164]. The values for all of the decay constants are listed in Table.I.

In the calculation of short-distance contributions, the weak transition form factors of Λ_c^+ to octet baryons are necessary inputs and have been investigated in the several QCD methods, such as Lattice QCD (LQCD) [165–168], light-front quark model (LFQM) [95, 169], light-cone sum rules (LCSR) [170], covariant quark model [171] and relativistic quark model [172]. Considering that the transition form factors from LQCD have higher accuracy, we use the calculation results with higher-order fit in [166, 167], see Table.II.

In addition, the strong coupling constants are crucial non-perturbative parameters in our calculation. For the strong couplings between octet baryons and light mesons, we use their values obtained with the method of LCSRs under the $SU(3)$ flavor symmetry [173, 174]. The couplings among decuplet baryons, octet baryons and light mesons are obtained from the experiment data about NN potential [175], that is $g_{\Delta N\pi}^2/(4\pi) = 0.36$ and $g_{\Delta N\rho}^2/(4\pi) = 20.45$, the rest of this type of couplings are derived from $SU(3)$ flavor symmetry. All of the three kinds of meson couplings are determined based on the exact $SU(3)$ flavor symmetry and the value of the couplings $g_{\rho\pi\pi}$, $g_{\rho\rho\rho}$, $g_{\omega\rho\pi}$. The coupling constant $g_{\rho\pi\pi} = 6.05 \pm 0.02$ quantifies how the ρ meson interacts with two pions,

TABLE II: The transition form factors of Λ_c^+ to octet baryons from the LQCD method [166, 167] and evolved to the physical region via BCL parameterization with high-order fit.

Decay	$f_1(0)$	$f_2(0)$	$g_1(0)$	$g_2(0)$
$\Lambda_c^+ \rightarrow \Lambda$ [166]	0.655 ± 0.022	-0.307 ± 0.042	0.578 ± 0.015	0.002 ± 0.030
$\Lambda_c^+ \rightarrow N$ [167]	0.662 ± 0.039	-0.322 ± 0.050	0.599 ± 0.031	-0.002 ± 0.053

extracted from experimental data [136]. The hidden local symmetry theory relates the $\rho\rho\rho$ coupling constant, $g_{\rho\rho\rho}$, to the ρ meson mass (m_ρ) and the pion physical decay constant ($F_\pi = 93\text{MeV}$), given by $g_{\rho\rho\rho} = \frac{m_\rho}{2F_\pi}$ [176]. Additionally, the coupling constant $g_{\omega\rho\pi}$ can be expressed as $g_{\omega\rho\pi} = \frac{3}{16\pi^2} g_{\rho\rho\rho}^2$, describing the interaction between the ω meson, ρ meson, and a pion [177].

B. Branching ratios

By summing the squares of all helicity amplitudes labeled by the spins of the initial and final states, and averaging over the initial state particle spins, we obtain the formula for the decay width

$$\Gamma(\mathcal{B}_c \rightarrow \mathcal{B}_8 V) = \frac{p_c}{8\pi m_i^2} \frac{1}{2} \sum_{\lambda_i \lambda_f \lambda_V} \left| H_{\lambda_f, \lambda_V}^{\lambda_i}(\mathcal{B}_c \rightarrow \mathcal{B}_8 V) \right|^2, \quad (42)$$

where $p_c = \frac{1}{2m_i} \sqrt{\left[m_i^2 - (m_f^2 + m_V^2) \right] \left[m_i^2 - (m_f^2 - m_V^2) \right]}$, m_i and m_f are the masses of the initial and final state baryons, m_V is the mass of vector mesons. λ_i , λ_f and λ_V label the helicity of the initial, final state baryon and the vector meson respectively. Then dividing by the total width of Λ_c we can get the branching ratio for each channel.

With the inputs discussed in last section, we obtain the branching fractions of $\Lambda_c \rightarrow \mathcal{B}_8 V$ as shown in Table.III, where the decay modes are classified into three categories (Cabbibo favoured (CF), single Cabbibo suppressed (SCS) and double Cabbibo suppressed (DCS)) according to CKM matrix element.

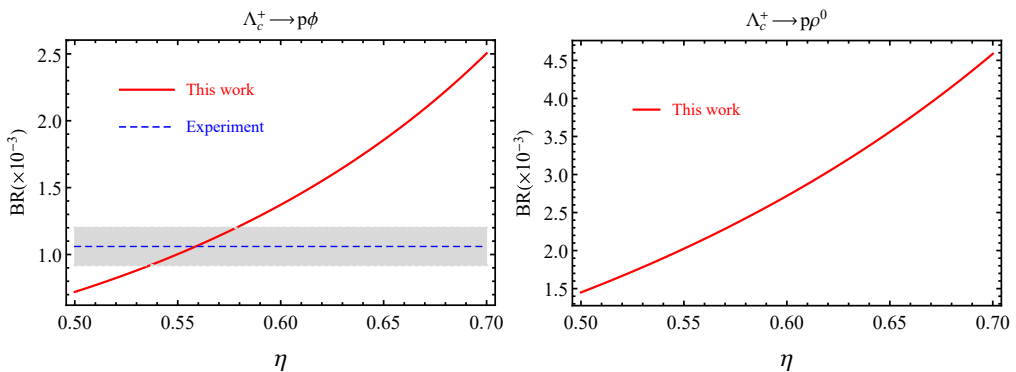
Based on the results in Table III, it is evident that the relative magnitudes of the factorizable contributions from the T and C diagrams are consistent with the relative sizes of their corresponding effective Wilson coefficients, in accordance with theoretical expectations. Moreover, for decay processes with the same decay mode, i.e., involving the same CKM matrix element, the decay branching ratios of processes that include T diagram and those that do not are of the same order of magnitude. This underscores the significant role of non-factorizable contributions in charmed baryon decays, which cannot be ignored. Additionally, for several processes with identical topological diagrams, the variations in their branching ratios are primarily due to the CKM matrix elements, further quantitatively confirming the universality of the topological diagram approach.

Using the process $\Lambda_c^+ \rightarrow \Lambda^0 \rho^+$ as an example, where short-distance contributions dominate, the decay width comprises both short and long-distance contributions, with the former being predominant. Consequently, the decay branching ratio exhibits a weak dependence on η . However, as η increases, the long-distance contribution also gradually increases, eventually becoming comparable to the short-distance contribution. At this point, the dependence of the decay branching ratio on the η parameter becomes stronger. The accompanying graph illustrates the dependence of the decay branching ratio on η for this process.

At $\eta = 0.6$, the contribution from long-distance effects rises to a point where it matches the contribution from short-distance effects. This results in a notable shift in the η dependence. The

TABLE III: The branching ratio of $\Lambda_c^+ \rightarrow \mathcal{B}_8 V$ processes with $\eta = 0.6 \pm 0.1$.

Decay modes	Topology	$\mathcal{B}R_{SD}(\%)$	$\mathcal{B}R_{LD}(\%)$	$\mathcal{B}R_{tot}(\%)$	$\mathcal{B}R_{exp}(\%)$
$\Lambda_c^+ \rightarrow \Lambda^0 \rho^+$	T, C', E_2, B	6.12	$2.30^{+1.18}_{-1.94}$	$6.26^{+2.44}_{-1.39}$	4.06 ± 0.52
$\Lambda_c^+ \rightarrow \Sigma^+ \rho^0$	C', E_2, B	—	—	$0.77^{+1.38}_{-0.53}$	< 1.7
$\Lambda_c^+ \rightarrow \Sigma^+ \omega$	C', E_2, B	—	—	$2.06^{+0.40}_{-1.78}$	1.7 ± 0.21
$\Lambda_c^+ \rightarrow \Sigma^+ \phi$	E_1	—	—	$0.33^{+0.08}_{-0.29}$	0.39 ± 0.06
$\Lambda_c^+ \rightarrow p\bar{K}^{*0}$	C, E_1	3.26×10^{-3}	$3.76^{+1.37}_{-3.43}$	$3.70^{+1.29}_{-3.39}$	1.96 ± 0.27
$\Lambda_c^+ \rightarrow \Xi^0 K^{*+}$	E_2, B	—	—	$1.94^{+0.40}_{-1.68}$	—
Decay modes	Topology	$\mathcal{B}R_{SD}(\times 10^{-3})$	$\mathcal{B}R_{LD}(\times 10^{-3})$	$\mathcal{B}R_{tot}(\times 10^{-3})$	$\mathcal{B}R_{exp}(\times 10^{-3})$
$\Lambda_c^+ \rightarrow \Lambda^0 K^{*+}$	T, C', E_2, B	2.92	$2.78^{+1.28}_{-1.02}$	$4.71^{+0.48}_{-0.20}$	—
$\Lambda_c^+ \rightarrow \Sigma^0 K^{*+}$	C', E_2, B	—	—	$1.60^{+0.89}_{-0.62}$	—
$\Lambda_c^+ \rightarrow \Sigma^+ K^{*0}$	C', E_1	—	—	$2.10^{+1.37}_{-0.86}$	3.5 ± 1.0
$\Lambda_c^+ \rightarrow p\phi$	C	1.78×10^{-3}	$1.44^{+1.14}_{-0.66}$	$1.37^{+1.13}_{-0.65}$	1.06 ± 0.14
$\Lambda_c^+ \rightarrow p\omega$	C, C', E_1, E_2, B	1.48×10^{-3}	$1.28^{+0.46}_{-0.37}$	$1.26^{+0.45}_{-0.37}$	0.83 ± 0.11
$\Lambda_c^+ \rightarrow p\rho^0$	C, C', E_1, E_2, B	1.81×10^{-3}	$2.79^{+1.89}_{-1.29}$	$2.72^{+1.87}_{-1.27}$	1.52 ± 0.44
$\Lambda_c^+ \rightarrow n\rho^+$	T, C', E_2, B	7.14	$8.50^{+9.57}_{-4.72}$	$26.39^{+13.71}_{-8.86}$	—
Decay modes	Topology	$\mathcal{B}R_{SD}(\times 10^{-4})$	$\mathcal{B}R_{LD}(\times 10^{-4})$	$\mathcal{B}R_{tot}(\times 10^{-4})$	$\mathcal{B}R_{exp}$
$\Lambda_c^+ \rightarrow pK^{*0}$	C, C'	9.28×10^{-4}	$0.53^{+3.67}_{-0.38}$	$0.55^{+3.71}_{-0.39}$	—
$\Lambda_c^+ \rightarrow nK^{*+}$	T, C'	3.66	$0.44^{+1.64}_{-0.30}$	$5.08^{+1.95}_{-0.66}$	—


 FIG. 5: The dependence of branching ratio on η for decay mode $\Lambda_c^+ \rightarrow p\phi$ and $p\rho^0$.

η parameter strongly influences the decay branching ratios across various processes. However, the sensitivity of the ratio of these branching ratios to η diminishes considerably.

In addition to the model parameter η , the observables of interest are influenced by non-perturbative input parameters such as heavy-to-light form factors and strong coupling constants. These parameters are typically determined using non-perturbative methods or extracted from experimental data, but they can carry significant uncertainties. The heavy-to-light form factors are particularly crucial as they appear in both short-distance and long-distance contributions. Their impact on the decay branching ratios, such as in the $\Lambda_c^+ \rightarrow \Lambda^0 \rho^+$ process, is substantial.

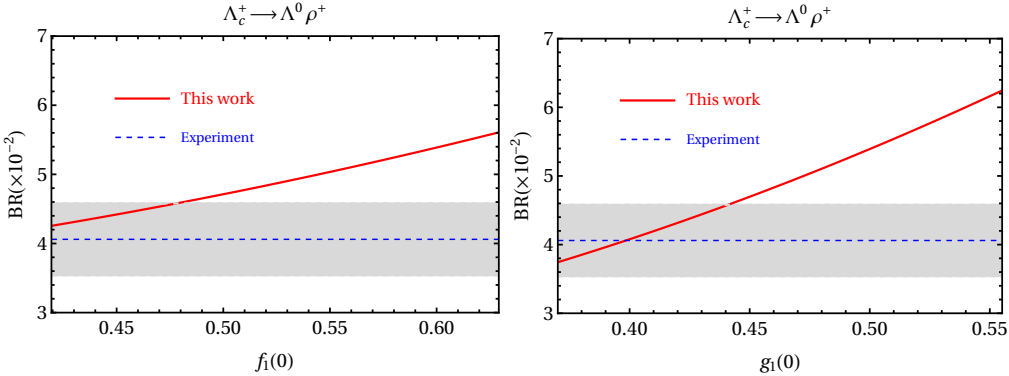


FIG. 6: The dependence of branching ratio on heavy to light form factors for decay mode $\Lambda_c^+ \rightarrow \Lambda^0 \rho^+$.

To illustrate, consider the dependence of the decay branching ratio on two significant $\Lambda_c \rightarrow \Lambda$ transition form factors, denoted as f_1 and g_1 . Graphically depicting this dependence helps visualize how variations in these form factors affect the overall branching ratio of the decay process. This sensitivity underscores the importance of accurately determining these form factors to improve the precision of theoretical predictions and to interpret experimental data effectively. In Fig.6, it is evident that the heavy-to-light form factor g_1 exerts a stronger influence on the decay branching ratio compared to f_1 , especially when considering variations within a 20% error margin. These form factors, derived from lattice QCD calculations, show discrepancies particularly in the low q^2 region where they tend to exceed experimental measurements. These discrepancies introduce significant uncertainties into the predicted decay branching ratio. Therefore, improving the precision of these form factor determinations, especially to better align with experimental data across different momentum transfer ranges, is crucial for enhancing the reliability of theoretical predictions for processes like $\Lambda_c^+ \rightarrow \Lambda^0 \rho^+$. This alignment is essential for reducing uncertainties and improving the reliability of theoretical models in describing such decay processes accurately.

The strong coupling constant plays a crucial role in theoretical calculations, especially in processes involving long-distance effects. Variations in its values from different theoretical approaches, as highlighted in [174], can lead to significant uncertainties, including the possibility of differences in sign. These variations directly translate into uncertainties in the predicted decay branching ratios of particles. In particular, the impact of the strong coupling constant is more pronounced for vertices involving vector particles compared to those involving pseudoscalar particles. This difference arises primarily due to the larger contributions from vector particle-related triangle diagrams in the decay processes. To illustrate this, let's consider the example of the $\Lambda_c^+ \rightarrow \Sigma^+ \phi$ decay process, where we analyze the effects of the strong coupling constants D_2 and F_2 associated with the $\mathcal{B}_8 \mathcal{B}_8 V$ vertex. When we adopt a 50% uncertainty in these coupling constants, the branching ratio of this decay process can vary significantly—up to 6 to 7 times. This sensitivity underscores the importance of accurately determining these strong coupling constants to reduce uncertainties in theoretical predictions. Thus, improving the precision of these non-perturbative parameters is crucial for refining theoretical models and ensuring they align closely with experimental observations, thereby enhancing our understanding of particle decay dynamics.

In certain decay channels, such as $\Lambda_c^+ \rightarrow \Sigma^+ \phi$ and $\Lambda_c^+ \rightarrow p\phi$, each involving a single topological diagram (denoted as E_1 and C respectively), the computed amplitude magnitude reflects the size of these diagrams. This characteristic allows for extracting information about the topological diagram itself. After normalizing for the effects of CKM matrix elements specific to the decay processes, the relative sizes of the E_1 and C diagrams are determined to lie between $0.5^{+0.2}_{-0.1}$ when

the parameter η varies from 0.5 to 0.7. This finding is consistent with analyses conducted using the SCET method. Additionally, the branching fractions of $\Lambda_c^+ \rightarrow p\omega$ and $\Lambda_c^+ \rightarrow p\rho^0$ determined from LHCb collaboration [178] are consistent with our calculations, as shown in Table III.

C. Decay parameters

The asymmetry parameters in the decay process $\Lambda_c^+ \rightarrow \mathcal{B}_8 V$ quantify differences in the magnitudes squared of various helicity amplitudes. This approach helps reduce the influence of the η parameter. Specifically, this decay involves four distinct non-zero helicity amplitudes. The BESIII experiment, as defined in the measurement methodology outlined by Hong et al. (2022) [179], defines several types of asymmetry parameters for measurement. These parameters play a crucial role in analyzing how decay events distribute across the final-state particles \mathcal{B}_8 and V , providing valuable insights into the angular correlations and dynamics of strong interactions within this decay process,

$$\alpha = \frac{\left|H_{1,\frac{1}{2}}\right|^2 - \left|H_{-1,-\frac{1}{2}}\right|^2}{\left|H_{1,\frac{1}{2}}\right|^2 + \left|H_{-1,-\frac{1}{2}}\right|^2}, \quad \beta = \frac{\left|H_{0,\frac{1}{2}}\right|^2 - \left|H_{0,-\frac{1}{2}}\right|^2}{\left|H_{0,\frac{1}{2}}\right|^2 + \left|H_{0,-\frac{1}{2}}\right|^2}, \quad \gamma = \frac{\left|H_{1,\frac{1}{2}}\right|^2 + \left|H_{-1,-\frac{1}{2}}\right|^2}{\left|H_{0,\frac{1}{2}}\right|^2 + \left|H_{0,-\frac{1}{2}}\right|^2}, \quad (43)$$

$$P_L = \frac{\left|H_{1,\frac{1}{2}}\right|^2 - \left|H_{-1,-\frac{1}{2}}\right|^2 + \left|H_{0,\frac{1}{2}}\right|^2 - \left|H_{0,-\frac{1}{2}}\right|^2}{\left|H_{1,\frac{1}{2}}\right|^2 + \left|H_{-1,-\frac{1}{2}}\right|^2 + \left|H_{0,\frac{1}{2}}\right|^2 + \left|H_{0,-\frac{1}{2}}\right|^2}. \quad (44)$$

these parameters are not all independent, they are related as follows,

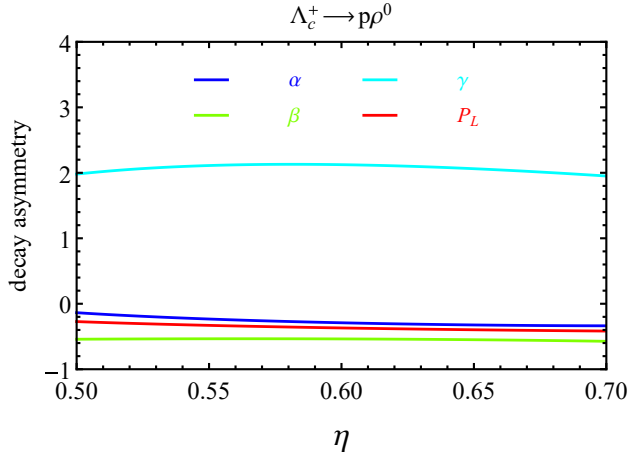
$$P_L = \frac{\beta + \alpha \cdot \gamma}{1 + \gamma}, \quad (45)$$

which can be used to check whether the results are correct. These definitions are related to the helicity amplitudes labeled by the expectation value of final state helicity as mentioned in Eq.(42). We calculated the decay asymmetry parameters with $\eta = 0.6 \pm 0.1$ and presented in Table.IV. The decay asymmetry parameters are the ratios of different linear combinations of helicity amplitudes, and therefore to some extent, they mitigate the dependence on model parameters and input parameters. Whether the process is dominated by short-distance contributions or long-distance contributions, the decay asymmetry parameter has a weaker dependence on the η parameter compared to the branching ratios. The curves in Fig.7 show the behavior of the four asymmetry parameters as the η parameter varies. It can be clearly seen that the asymmetry parameters show a slight dependency on the η parameter. Theoretical calculations of these parameters for $\Lambda_c^+ \rightarrow \Lambda^0 \rho^+$ closely match experimental measurements, indicating that the computed relative magnitudes and phases of helicity amplitudes are consistent with observations.

Similar to how the asymmetry parameters respond to changes in the η parameter, their sensitivity to variations in the heavy-to-light form factors is notably reduced. The graph illustrates a minimal correlation between the asymmetry parameters and the f_1 and g_1 form factors during the $\Lambda_c \rightarrow \Lambda$ transition, aligning closely with theoretical predictions. Likewise, the overall impact of the strong coupling constants on these decay asymmetry parameters is also significantly diminished, indicating a weak dependence on these coupling constants.

TABLE IV: The decay asymmetry parameters of $\Lambda_c^+ \rightarrow \mathcal{B}_8 V$ processes with $\eta = 0.6 \pm 0.1$.

Decay modes	α	β	γ	P_L
$\Lambda_c^+ \rightarrow \Lambda^0 \rho^+$	$-0.30^{+0.45}_{-0.40}$	$-0.67^{+0.06}_{-0.28}$	$0.30^{+0.20}_{-0.19}$	$-0.58^{+0.06}_{-0.28}$
$\Lambda_c^+ \rightarrow \Sigma^+ \rho^0$	$-0.82^{+0.04}_{-0.17}$	$-0.54^{+0.08}_{-0.02}$	$0.74^{+0.95}_{-0.14}$	$-0.66^{+0.05}_{-0.16}$
$\Lambda_c^+ \rightarrow \Sigma^+ \omega$	$0.85^{+0.002}_{-0.07}$	$0.58^{+0.12}_{-0.001}$	$3.27^{+1.17}_{-1.17}$	$0.81^{+0.02}_{-0.07}$
$\Lambda_c^+ \rightarrow \Sigma^+ \phi$	$-0.11^{+0.002}_{-0.03}$	$0.47^{+0.11}_{-0.10}$	$2.12^{+0.08}_{-0.06}$	$0.08^{+0.04}_{-0.05}$
$\Lambda_c^+ \rightarrow p \bar{K}^{*0}$	$0.15^{+0.01}_{-0.15}$	$0.73^{+0.21}_{-0.52}$	$3.15^{+1.35}_{-0.02}$	$0.29^{+0.19}_{-0.12}$
$\Lambda_c^+ \rightarrow \Xi^0 K^{*+}$	$-0.12^{+0.06}_{-0.15}$	$-0.03^{+0.03}_{-0.005}$	$1.56^{+0.14}_{-0.03}$	$-0.08^{+0.05}_{-0.10}$
$\Lambda_c^+ \rightarrow \Lambda^0 K^{*+}$	$-0.77^{+0.14}_{-0.08}$	$-0.39^{+0.25}_{-0.22}$	$1.54^{+0.21}_{-0.27}$	$-0.62^{+0.17}_{-0.13}$
$\Lambda_c^+ \rightarrow \Sigma^0 K^{*+}$	$-0.03^{+0.02}_{-0.01}$	$0.31^{+0.04}_{-0.07}$	$2.21^{+0.48}_{-0.33}$	$0.08^{+0.04}_{-0.03}$
$\Lambda_c^+ \rightarrow \Sigma^+ K^{*0}$	$0.07^{+0.06}_{-0.004}$	$0.40^{+0.02}_{-0.03}$	$1.52^{+0.08}_{-0.07}$	$0.20^{+0.02}_{-0.01}$
$\Lambda_c^+ \rightarrow p \phi$	$-0.11^{+0.06}_{-0.004}$	$-0.16^{+0.12}_{-0.07}$	$5.98^{+1.07}_{-0.76}$	$-0.12^{+0.07}_{-0.01}$
$\Lambda_c^+ \rightarrow p \omega$	$0.31^{+0.14}_{-1.02}$	$0.08^{+0.04}_{-0.05}$	$0.12^{+0.17}_{-0.06}$	$0.11^{+0.02}_{-0.11}$
$\Lambda_c^+ \rightarrow p \rho^0$	$-0.29^{+0.15}_{-0.05}$	$-0.54^{+0.01}_{-0.04}$	$2.12^{+0.14}_{-0.17}$	$-0.37^{+0.10}_{-0.05}$
$\Lambda_c^+ \rightarrow n \rho^+$	$-0.95^{+0.003}_{-0.004}$	$-0.61^{+0.14}_{-0.11}$	$0.36^{+0.01}_{-0.01}$	$-0.70^{+0.10}_{-0.08}$
$\Lambda_c^+ \rightarrow p K^{*0}$	$0.45^{+0.07}_{-0.14}$	$-0.27^{+0.48}_{-0.16}$	$9.87^{+3.61}_{-3.64}$	$0.39^{+0.09}_{-0.18}$
$\Lambda_c^+ \rightarrow n K^{*+}$	$-0.89^{+0.29}_{-0.05}$	$-0.83^{+0.37}_{-0.10}$	$1.04^{+0.34}_{-0.14}$	$-0.86^{+0.32}_{-0.07}$


 FIG. 7: The dependence of decay asymmetry parameters on η for decay mode $\Lambda_c^+ \rightarrow p \rho^0$.

D. CP asymmetries

In this part, we present the numerical predictions on direct CP violation in charmed baryon decays, which is a crucial aspect in understanding the asymmetry between matter and antimatter

TABLE V: The CP asymmetries ($\times 10^{-4}$) of $\Lambda_c^+ \rightarrow \mathcal{B}_8 V$ processes with $\eta = 0.6 \pm 0.1$.

Decay modes	A_{CP}^{dir}	α_{CP}	β_{CP}	γ_{CP}	$P_{L,CP}$
$\Lambda_c^+ \rightarrow \Lambda^0 K^{*+}$	$0.89_{-0.61}^{+0.91}$	$-0.84_{-0.97}^{+0.62}$	$-2.12_{-8.07}^{+1.60}$	$0.61_{-0.31}^{+0.40}$	$-1.07_{-1.43}^{+0.77}$
$\Lambda_c^+ \rightarrow \Sigma^0 K^{*+}$	$2.28_{-0.85}^{+0.92}$	$13.75_{-2.24}^{+18.22}$	$2.55_{-0.76}^{+2.02}$	$-1.00_{-0.50}^{+0.18}$	$0.69_{-0.89}^{+2.28}$
$\Lambda_c^+ \rightarrow \Sigma^+ K^{*0}$	$-1.99_{-0.74}^{+0.80}$	$5.51_{-1.11}^{+0.06}$	$0.95_{-0.20}^{+0.02}$	$0.64_{-0.05}^{+0.08}$	$1.64_{-0.18}^{+0.26}$
$\Lambda_c^+ \rightarrow p\omega$	$4.55_{-0.81}^{+0.36}$	$19.61_{-9.35}^{+8.95}$	$-14.80_{-1.99}^{+0.30}$	$8.32_{-8.17}^{+0.28}$	$-2.16_{-2.21}^{+0.01}$
$\Lambda_c^+ \rightarrow p\rho^0$	$3.73_{-1.16}^{+0.95}$	$0.48_{-0.98}^{+0.54}$	$2.88_{-0.71}^{+0.09}$	$-1.23_{-0.42}^{+0.90}$	$1.77_{-0.05}^{+0.20}$
$\Lambda_c^+ \rightarrow n\rho^+$	$-1.45_{-0.52}^{+0.29}$	$0.01_{-0.07}^{+0.32}$	$1.86_{-1.00}^{+1.34}$	$-1.21_{-0.01}^{+0.40}$	$1.08_{-0.59}^{+0.71}$

in the universe. The direct CP asymmetry is defined as follows

$$A_{CP}^{\text{dir}}(\Lambda_c^+ \rightarrow p\rho^0) = \frac{\Gamma(\Lambda_c^+ \rightarrow p\rho^0) - \bar{\Gamma}(\Lambda_c^+ \rightarrow p\rho^0)}{\Gamma(\Lambda_c^+ \rightarrow p\rho^0) + \bar{\Gamma}(\Lambda_c^+ \rightarrow p\rho^0)} = \frac{2r \sin \Delta\delta \sin \Delta\phi}{1 + r^2 + 2r \cos \Delta\delta \cos \Delta\phi}, \quad (46)$$

where r is the ratio of amplitudes, $\Delta\delta$ and $\Delta\phi$ are the strong and weak phase difference respectively.

Apart from this, there exist CP asymmetries induced by decay asymmetry parameters,

$$\alpha_{CP} = \frac{\alpha + \bar{\alpha}}{\alpha - \bar{\alpha}}, \quad \beta_{CP} = \frac{\beta + \bar{\beta}}{\beta - \bar{\beta}}, \quad \gamma_{CP} = \frac{\gamma - \bar{\gamma}}{\gamma + \bar{\gamma}}, \quad P_{L,CP} = \frac{P_L - \bar{P}_L}{P_L + \bar{P}_L}. \quad (47)$$

With the parameter $\eta = 0.6 \pm 0.1$ is adopted, the predictions of CP violations for charmed baryon decays are presented in Table V.

Due to the significantly suppressed CKM matrix elements associated with penguin operators, this study exclusively considers CP violation induced by tree-level operators. Specifically, for singly Cabibbo suppressed processes, two types of CKM matrix elements are involved: $V_{cd}V_{ud}^*$ and $V_{cs}V_{us}^*$. In the rescattering mechanism framework, both types contribute to the same process, generating a non-zero weak phase difference. Moreover, the long-distance final state interactions provide strong phase information for the decay process. Thus, our theoretical approach naturally computes the magnitude of CP violation and currently stands as the sole method capable of quantifying CP violation in charmed baryon decays. With the decay amplitude written as $\mathcal{A} = \lambda_d \mathcal{A}_d + \lambda_s \mathcal{A}_s$, $\lambda_q = V_{cq}V_{uq}^*$, $q = d, s$, the CP violation can then be expressed as

$$A_{CP}^{\text{dir}} \approx -2 \frac{\text{Im}(\lambda_d^* \lambda_s)}{|\lambda_d|^2} \frac{\text{Im}(\mathcal{A}_d^* \mathcal{A}_s)}{|\mathcal{A}_d - \mathcal{A}_s|^2}. \quad (48)$$

As displayed in Eq.(46), the direct CP violation is proportional to $\sin \Delta\phi$, where $\Delta\phi$ represents the weak phase difference, for tree-level operators in charmed baryon decays, $\Delta\phi = \arctan \left[\frac{\text{Im}(V_{cd})}{\text{Re}(V_{cd})} \right] \sim 6 \times 10^{-4}$. Consequently, the anticipated magnitude of CP violation in charmed baryon decays is expected to align with this level, consistent with the theoretical predictions in Table V.

For instance, the decay channel $\Lambda_c^+ \rightarrow p\rho^0$ involves CP violation induced by tree-level operators mediated by CKM matrix elements $V_{cd}V_{ud}$ and $V_{cs}V_{us}$. These elements contribute to the triangle diagram amplitudes depicted in Fig.8 and 9, influencing the decay amplitude and introducing a weak phase difference $\Delta\phi$. This phase difference, combining with the strong phases introduced

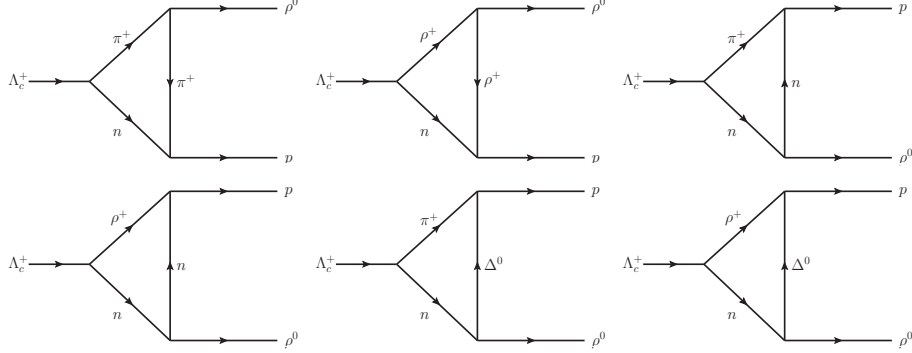


FIG. 8: The triangle diagrams for $\Lambda_c^+ \rightarrow p\rho^0$ with CKM matrix element $V_{cd}^* V_{ud}$.

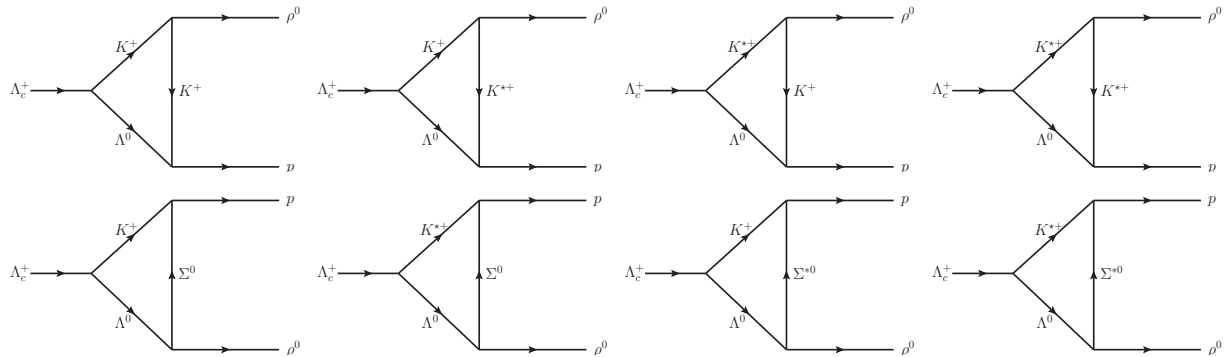


FIG. 9: The triangle diagrams for $\Lambda_c^+ \rightarrow p\rho^0$ with CKM matrix element $V_{cs}^* V_{us}$.

from the triangle integrals, is critical for understanding and predicting CP violation in charmed baryon decays.

To demonstrate the reliability of the theoretical method in predicting the magnitude of CP violation, it is crucial to analyze the dependence of CP violation parameters on model parameters, such as η . In the decay $\Lambda_c^+ \rightarrow p\rho^0$, the variation of CP violation parameters with respect to the η parameter is illustrated in Fig.10. This analysis helps establish how sensitive CP violation effects are to changes in the model parameter η . The observation that both direct CP violation and asymmetry parameter-induced CP violation exhibit very weak dependence on model parameters. It suggests that the predictions for CP violation observables are minimally affected by variations in the underlying theoretical assumptions or model parameters. Such findings are crucial for validating the theoretical approach and ensuring that the predicted magnitudes of CP violation are trustworthy and reflective of the physical processes involved in these decays.

V. SUMMARY

In this work, we seriously treated the final-state interaction effects in charmed baryon decay, due to its importance for understanding the dynamics of non-perturbative contributions at the charm scale. The calculations of the long-distance final state interactions are improved with a comprehensive treatment of hadronic-loop diagrams, rather than the Cutkosky rule which computed the imaginary parts of amplitudes barely. In the improved method, the complete real and imaginary parts of the amplitudes have been simultaneously calculated, so that it provides the strong phase to calculate the CP asymmetries. By accurately incorporating long-distance

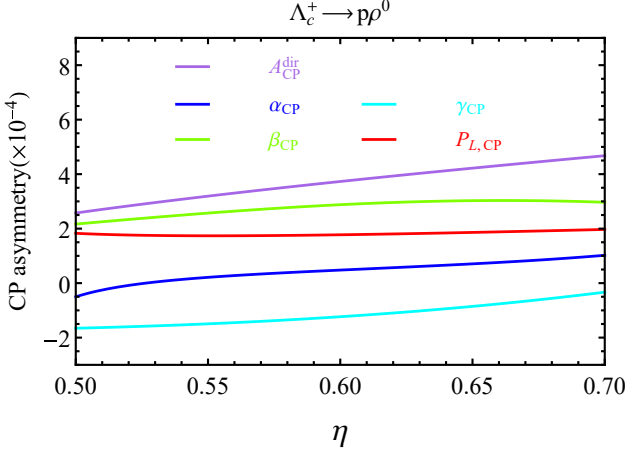


FIG. 10: The dependence of CP asymmetries on η for decay mode $\Lambda_c^+ \rightarrow p\rho^0$.

final state interactions, our method allows for precise predictions of decay observables for charmed baryon decays. The results within this method successfully matches experimental data of branching ratio across various decay channels such as $\Lambda_c^+ \rightarrow \mathcal{B}_8 V$. Furthermore, the decay asymmetries and CP asymmetries, being defined as ratios, exhibit very weak dependence on model parameters.

Moreover, our approach holds potential beyond charmed baryon decays, potentially extending to the study of weak decays in other heavy-flavor hadrons. Future advancements will focus on refining form factor treatments to further enhance predictive accuracy and reduce remaining model dependencies. This work thus represents a significant step forward in theoretical modeling of heavy-flavor hadron decays and CP violation phenomena.

Acknowledgments

The authors are grateful to Hai-Yang Cheng and Cai-Dian Lü for the useful discussions on the analysis of final-state interaction. Cai-Ping Jia is also grateful to Jia-Jie Han and Ming-Xiao Duan for the discussions of program. This work is supported in part by Natural Science Foundation of China under grant No. 12335003 and 12405114, and by the Fundamental Research Funds for the Central Universities under No. lzujbky-2024-oy02 and lzujbky-2021-it11.

Appendix A: Amplitudes of each modes

1. Cabibbo-favored

$$\begin{aligned}
\mathcal{A}(\Lambda_c^+ \rightarrow \Lambda^0 \rho^+) &= \mathcal{T}_{SD}(\Lambda_c^+ \rightarrow \Lambda^0 \rho^+) + \mathcal{M}(\pi^+, \Lambda^0; \omega) + \mathcal{M}(\rho^+, \Lambda^0; \eta_8) + \mathcal{M}(\rho^+, \Lambda^0; \eta_1) \\
&\quad + \mathcal{M}(\pi^+, \Lambda^0; \Sigma^-) + \mathcal{M}(\rho^+, \Lambda^0; \Sigma^-) + \mathcal{M}(\pi^+, \Lambda^0; \Sigma^{*-}) + \mathcal{M}(\rho^+, \Lambda^0; \Sigma^{*-}) \\
\mathcal{A}(\Lambda_c^+ \rightarrow \Sigma^+ \rho^0) &= \mathcal{M}(\pi^+, \Lambda^0; \pi^+) + \mathcal{M}(\rho^+, \Lambda^0; \rho^+) + \mathcal{M}(\pi^+, \Lambda^0; \Sigma^0) + \mathcal{M}(\rho^+, \Lambda^0; \Sigma^0) \\
&\quad + \mathcal{M}(\pi^+, \Lambda^0; \Sigma^{*0}) + \mathcal{M}(\rho^+, \Lambda^0; \Sigma^{*0}) \\
\mathcal{A}(\Lambda_c^+ \rightarrow \Sigma^0 \rho^+) &= \mathcal{M}(\pi^+, \Lambda^0; \pi^0) + \mathcal{M}(\rho^+, \Lambda^0; \rho^0) \\
&\quad + \mathcal{M}(\pi^+, \Lambda^0; \Sigma^-) + \mathcal{M}(\rho^+, \Lambda^0; \Sigma^-) + \mathcal{M}(\pi^+, \Lambda^0; \Sigma^{*-}) + \mathcal{M}(\rho^+, \Lambda^0; \Sigma^{*-})
\end{aligned}$$

$$\mathcal{A}(\Lambda_c^+ \rightarrow \Sigma^+ \omega) = \mathcal{M}(\pi^+, \Lambda^0; \rho^+) + \mathcal{M}(\rho^+, \Lambda^0; \pi^+) + \mathcal{M}(\pi^+, \Lambda^0; \Lambda^0) + \mathcal{M}(\rho^+, \Lambda^0; \Lambda^0)$$

$$\mathcal{A}(\Lambda_c^+ \rightarrow \Sigma^+ \phi) = \mathcal{M}(\pi^+, \Lambda^0; \Lambda^0) + \mathcal{M}(\rho^+, \Lambda^0; \Lambda^0)$$

$$\begin{aligned} \mathcal{A}(\Lambda_c^+ \rightarrow p\bar{K}^{*0}) = & \mathcal{C}_{SD}(\Lambda_c^+ \rightarrow p\bar{K}^{*0}) + \mathcal{M}(\pi^+, \Lambda^0; K^+) + \mathcal{M}(\pi^+, \Lambda^0; K^{*+}) + \mathcal{M}(\rho^+, \Lambda^0; K^+) \\ & + \mathcal{M}(\rho^+, \Lambda^0; K^{*+}) + \mathcal{M}(\pi^+, \Lambda^0; n) + \mathcal{M}(\rho^+, \Lambda^0; n) \end{aligned}$$

$$\begin{aligned} \mathcal{A}(\Lambda_c^+ \rightarrow \Xi^0 K^{*+}) = & \mathcal{M}(\pi^+, \Lambda^0; \bar{K}^0) + \mathcal{M}(\pi^+, \Lambda^0; \bar{K}^{*0}) + \mathcal{M}(\rho^+, \Lambda^0; \bar{K}^0) + \mathcal{M}(\rho^+, \Lambda^0; \bar{K}^{*0}) \\ & + \mathcal{M}(\pi^+, \Lambda^0; \Xi^-) + \mathcal{M}(\rho^+, \Lambda^0; \Xi^-) + \mathcal{M}(\pi^+, \Lambda^0; \Xi^{*-}) + \mathcal{M}(\rho^+, \Lambda^0; \Xi^{*-}) \end{aligned}$$

2. Singly Cabibbo-suppressed

$$\begin{aligned} \mathcal{A}(\Lambda_c^+ \rightarrow \Lambda^0 K^{*+}) = & \mathcal{T}_{SD}(\Lambda_c^+ \rightarrow \Lambda^0 K^{*+}) + \mathcal{M}(\pi^+, n; \bar{K}^0) + \mathcal{M}(\pi^+, n; \bar{K}^{*0}) + \mathcal{M}(\rho^+, n; \bar{K}^0) \\ & + \mathcal{M}(\rho^+, n; \bar{K}^{*0}) + \mathcal{M}(\pi^+, n; \Sigma^-) + \mathcal{M}(\rho^+, n; \Sigma^-) + \mathcal{M}(\pi^+, n; \Sigma^{*-}) + \mathcal{M}(\rho^+, n; \Sigma^{*-}) \\ & + \mathcal{M}(K^+, \Lambda^0; \eta_8) + \mathcal{M}(K^+, \Lambda^0; \eta_1) + \mathcal{M}(K^+, \Lambda^0; \omega) + \mathcal{M}(K^+, \Lambda^0; \phi) \\ & + \mathcal{M}(K^{*+}, \Lambda^0; \eta_8) + \mathcal{M}(K^{*+}, \Lambda^0; \eta_1) + \mathcal{M}(K^{*+}, \Lambda^0; \omega) + \mathcal{M}(K^{*+}, \Lambda^0; \phi) \\ & + \mathcal{M}(K^+, \Lambda^0; \Xi^-) + \mathcal{M}(K^{*+}, \Lambda^0; \Xi^-) + \mathcal{M}(K^+, \Lambda^0; \Xi^{*-}) + \mathcal{M}(K^{*+}, \Lambda^0; \Xi^{*-}) \end{aligned}$$

$$\begin{aligned} \mathcal{A}(\Lambda_c^+ \rightarrow \Sigma^0 K^{*+}) = & \mathcal{M}(\pi^+, n; \bar{K}^0) + \mathcal{M}(\pi^+, n; \bar{K}^{*0}) + \mathcal{M}(\rho^+, n; \bar{K}^0) + \mathcal{M}(\rho^+, n; \bar{K}^{*0}) \\ & + \mathcal{M}(\pi^+, n; \Sigma^-) + \mathcal{M}(\rho^+, n; \Sigma^-) + \mathcal{M}(\pi^+, n; \Sigma^{*-}) + \mathcal{M}(\rho^+, n; \Sigma^{*-}) \\ & + \mathcal{M}(K^+, \Lambda^0; \rho^0) + \mathcal{M}(K^+, \Lambda^0; \rho^0) + \mathcal{M}(K^{*+}, \Lambda^0; \rho^0) + \mathcal{M}(K^{*+}, \Lambda^0; \rho^0) \\ & + \mathcal{M}(K^+, \Lambda^0; \Xi^-) + \mathcal{M}(K^{*+}, \Lambda^0; \Xi^-) + \mathcal{M}(K^+, \Lambda^0; \Xi^{*-}) + \mathcal{M}(K^{*+}, \Lambda^0; \Xi^{*-}) \end{aligned}$$

$$\begin{aligned} \mathcal{A}(\Lambda_c^+ \rightarrow \Sigma^+ K^{*0}) = & \mathcal{M}(\pi^+, n; \Lambda^0) + \mathcal{M}(\rho^+, n; \Lambda^0) + \mathcal{M}(\pi^+, n; \Sigma^0) + \mathcal{M}(\rho^+, n; \Sigma^0) + \mathcal{M}(\pi^+, n; \Sigma^{*0}) \\ & + \mathcal{M}(\rho^+, n; \Sigma^{*0}) + \mathcal{M}(K^+, \Lambda^0; \pi^+) + \mathcal{M}(K^+, \Lambda^0; \rho^+) + \mathcal{M}(K^{*+}, \Lambda^0; \pi^+) \\ & + \mathcal{M}(K^{*+}, \Lambda^0; \rho^+) + \mathcal{M}(K^+, \Lambda^0; \Xi^0) + \mathcal{M}(K^{*+}, \Lambda^0; \Xi^0) + \mathcal{M}(K^+, \Lambda^0; \Xi^{*0}) \\ & + \mathcal{M}(K^{*+}, \Lambda^0; \Xi^{*0}) \end{aligned}$$

$$\begin{aligned} \mathcal{A}(\Lambda_c^+ \rightarrow p\phi) = & \mathcal{C}_{SD}(\Lambda_c^+ \rightarrow p\phi) + \mathcal{M}(K^+, \Lambda^0; K^+) + \mathcal{M}(K^+, \Lambda^0; K^{*+}) + \mathcal{M}(K^{*+}, \Lambda^0; K^+) \\ & + \mathcal{M}(K^{*+}, \Lambda^0; K^{*+}) + \mathcal{M}(K^+, \Lambda^0; \Lambda^0) + \mathcal{M}(K^{*+}, \Lambda^0; \Lambda^0) \end{aligned}$$

$$\begin{aligned} \mathcal{A}(\Lambda_c^+ \rightarrow p\omega) = & \mathcal{C}_{SD}(\Lambda_c^+ \rightarrow p\omega) + \mathcal{M}(\pi^+, n; \rho^+) + \mathcal{M}(\rho^+, n; \pi^+) + \mathcal{M}(\pi^+, n; n) + \mathcal{M}(\rho^+, n; n) \\ & + \mathcal{M}(K^+, \Lambda^0; K^+) + \mathcal{M}(K^+, \Lambda^0; K^{*+}) + \mathcal{M}(K^{*+}, \Lambda^0; K^+) + \mathcal{M}(K^{*+}, \Lambda^0; K^{*+}) \\ & + \mathcal{M}(K^+, \Lambda^0; \Lambda^0) + \mathcal{M}(K^{*+}, \Lambda^0; \Lambda^0) \end{aligned}$$

$$\begin{aligned} \mathcal{A}(\Lambda_c^+ \rightarrow p\rho^0) = & \mathcal{C}_{SD}(\Lambda_c^+ \rightarrow p\rho^0) + \mathcal{M}(\pi^+, n; \pi^+) + \mathcal{M}(\rho^+, n; \rho^+) + \mathcal{M}(\pi^+, n; n) + \mathcal{M}(\rho^+, n; n) \\ & + \mathcal{M}(\pi^+, n; \Delta^0) + \mathcal{M}(\rho^+, n; \Delta^0) + \mathcal{M}(K^+, \Lambda^0; K^+) + \mathcal{M}(K^+, \Lambda^0; K^{*+}) \\ & + \mathcal{M}(K^{*+}, \Lambda^0; K^+) + \mathcal{M}(K^{*+}, \Lambda^0; K^{*+}) + \mathcal{M}(K^+, \Lambda^0; \Sigma^0) + \mathcal{M}(K^{*+}, \Lambda^0; \Sigma^0) \\ & + \mathcal{M}(K^+, \Lambda^0; \Sigma^{*0}) + \mathcal{M}(K^{*+}, \Lambda^0; \Sigma^{*0}) \end{aligned}$$

$$\begin{aligned}
\mathcal{A}(\Lambda_c^+ \rightarrow n\rho^+) = & \mathcal{T}_{SD}(\Lambda_c^+ \rightarrow n\rho^+) + \mathcal{M}(\pi^+, n; \pi^0) + \mathcal{M}(\rho^+, n; \rho^0) + \mathcal{M}(\pi^+, n; \omega) \\
& + \mathcal{M}(\rho^+, n; \eta_8) + \mathcal{M}(\rho^+, n; \eta_1) + \mathcal{M}(\pi^+, n; \Delta^-) + \mathcal{M}(\rho^+, n; \Delta^-) \\
& + \mathcal{M}(K^+, \Lambda^0; K^0) + \mathcal{M}(K^+, \Lambda^0; K^{*0}) + \mathcal{M}(K^{*+}, \Lambda^0; K^0) + \mathcal{M}(K^{*+}, \Lambda^0; K^{*0}) \\
& + \mathcal{M}(K^+, \Lambda^0; \Sigma^-) + \mathcal{M}(K^{*+}, \Lambda^0; \Sigma^-) + \mathcal{M}(K^+, \Lambda^0; \Sigma^{*-}) + \mathcal{M}(K^{*+}, \Lambda^0; \Sigma^{*-})
\end{aligned}$$

3. Doubly Cabibbo-suppressed

$$\begin{aligned}
\mathcal{A}(\Lambda_c^+ \rightarrow pK^{*0}) = & \mathcal{C}_{SD}(\Lambda_c^+ \rightarrow pK^{*0}) + \mathcal{M}(K^+, n; \pi^+) + \mathcal{M}(K^+, n; \rho^+) + \mathcal{M}(K^{*+}, n; \pi^+) \\
& + \mathcal{M}(K^{*+}, n; \rho^+) + \mathcal{M}(K^+, n; \Lambda^0) + \mathcal{M}(K^{*+}, n; \Lambda^0) + \mathcal{M}(K^+, n; \Sigma^0) \\
& + \mathcal{M}(K^{*+}, n; \Sigma^0) + \mathcal{M}(K^+, n; \Sigma^{*0}) + \mathcal{M}(K^{*+}, n; \Sigma^{*0})
\end{aligned}$$

$$\begin{aligned}
\mathcal{A}(\Lambda_c^+ \rightarrow nK^{*+}) = & \mathcal{T}_{SD}(\Lambda_c^+ \rightarrow nK^{*+}) + \mathcal{M}(K^+, n; \pi^0) + \mathcal{M}(K^+, n; \eta_8) + \mathcal{M}(K^+, n; \eta_1) \\
& + \mathcal{M}(K^+, n; \rho^0) + \mathcal{M}(K^+, n; \omega) + \mathcal{M}(K^{*+}, n; \pi^0) + \mathcal{M}(K^{*+}, n; \eta_8) \\
& + \mathcal{M}(K^{*+}, n; \eta_1) + \mathcal{M}(K^{*+}, n; \rho^0) + \mathcal{M}(K^{*+}, n; \omega) + \mathcal{M}(K^+, n; \Sigma^-) \\
& + \mathcal{M}(K^{*+}, n; \Sigma^-) + \mathcal{M}(K^+, n; \Sigma^{*-}) + \mathcal{M}(K^{*+}, n; \Sigma^{*-})
\end{aligned}$$

Appendix B: Effective Lagrangian

The effective Lagrangian used in the re-scattering mechanism are [137, 173, 174, 180, 181]

$$\begin{aligned}
\mathcal{L}_{VPP} &= \frac{i g_{\rho\pi\pi}}{\sqrt{2}} Tr [V^\mu [P, \partial_\mu P]] \\
\mathcal{L}_{VVV} &= \frac{i g_{\rho\rho\rho}}{\sqrt{2}} Tr [(\partial_\nu V_\mu V^\mu - V_\mu \partial_\nu V^\mu) V^\nu] \\
\mathcal{L}_{VVP} &= \frac{4 g_{VVP}}{f_P} \epsilon^{\mu\nu\alpha\beta} Tr [\partial_\mu V_\nu \partial_\alpha V_\beta P] \\
\mathcal{L}_{\mathcal{B}_8\mathcal{B}_8P} &= \sqrt{2} D Tr [\bar{\mathcal{B}}_8 i \gamma_5 \{P, \mathcal{B}_8\}] + \sqrt{2} F Tr [\bar{\mathcal{B}}_8 i \gamma_5 [P, \mathcal{B}_8]] \quad (B1) \\
\mathcal{L}_{\mathcal{B}_8\mathcal{B}_8V} &= \sqrt{2} D' Tr [\bar{\mathcal{B}}_8 \gamma_\mu \{V^\mu, \mathcal{B}_8\}] + \sqrt{2} F' Tr [\bar{\mathcal{B}}_8 \gamma_\mu [V^\mu, \mathcal{B}_8]] \\
&\quad - \sqrt{2} (D' - F') Tr (\bar{\mathcal{B}}_8 \gamma_\mu \mathcal{B}_8) Tr V^\mu \\
\mathcal{L}_{\mathcal{B}_{10}\mathcal{B}_8P} &= \frac{g_{\Delta N\pi}}{m_\pi} \epsilon_{ijk} (\bar{\mathcal{B}}_8)_l^j (\mathcal{B}_{10})_\mu^{mkl} \partial^\mu P_m^i \\
\mathcal{L}_{\mathcal{B}_{10}\mathcal{B}_8V} &= -i \frac{g_{\rho N\Delta}}{m_\rho} [(\bar{\mathcal{B}}_{10})^\mu \gamma^5 \gamma^\nu \mathcal{B}_8 + \bar{\mathcal{B}}_8 \gamma^5 \gamma^\nu (\mathcal{B}_{10})^\mu] (\partial_\mu \rho_\nu - \partial_\nu \rho_\mu)
\end{aligned}$$

where the corresponding $V, P, \mathcal{B}_8, \mathcal{B}_{10}$ represent the vector and pseudo-scalar meson octet, baryon octet and decuplet respectively under $SU(3)$ flavor group.

[1] A. D. Sakharov, Violation of CP Invariance, C asymmetry, and baryon asymmetry of the universe, Pisma Zh. Eksp. Teor. Fiz. 5 (1967) 32–35. doi:10.1070/PU1991v03n05ABEH002497.

- [2] M. Beneke, G. Buchalla, M. Neubert, C. T. Sachrajda, QCD factorization for $B \rightarrow \pi \pi$ decays: Strong phases and CP violation in the heavy quark limit, Phys. Rev. Lett. 83 (1999) 1914–1917. doi:10.1103/PhysRevLett.83.1914. arXiv:hep-ph/9905312.
- [3] M. Beneke, G. Buchalla, M. Neubert, C. T. Sachrajda, QCD factorization for exclusive, nonleptonic B meson decays: General arguments and the case of heavy light final states, Nucl. Phys. B 591 (2000) 313–418. doi:10.1016/S0550-3213(00)00559-9. arXiv:hep-ph/0006124.
- [4] M. Beneke, G. Buchalla, M. Neubert, C. T. Sachrajda, QCD factorization in $B \rightarrow \pi K$, $\pi \pi$ decays and extraction of Wolfenstein parameters, Nucl. Phys. B 606 (2001) 245–321. doi:10.1016/S0550-3213(01)00251-6. arXiv:hep-ph/0104110.
- [5] M. Beneke, M. Neubert, QCD factorization for $B \rightarrow PP$ and $B \rightarrow PV$ decays, Nucl. Phys. B 675 (2003) 333–415. doi:10.1016/j.nuclphysb.2003.09.026. arXiv:hep-ph/0308039.
- [6] Y. Y. Keum, H.-N. Li, A. I. Sanda, Penguin enhancement and $B \rightarrow K\pi$ decays in perturbative QCD, Phys. Rev. D 63 (2001) 054008. doi:10.1103/PhysRevD.63.054008. arXiv:hep-ph/0004173.
- [7] Y.-Y. Keum, H.-n. Li, A. I. Sanda, Fat penguins and imaginary penguins in perturbative QCD, Phys. Lett. B 504 (2001) 6–14. doi:10.1016/S0370-2693(01)00247-7. arXiv:hep-ph/0004004.
- [8] C.-D. Lu, K. Ukai, M.-Z. Yang, Branching ratio and CP violation of $B \rightarrow \pi \pi$ decays in perturbative QCD approach, Phys. Rev. D 63 (2001) 074009. doi:10.1103/PhysRevD.63.074009. arXiv:hep-ph/0004213.
- [9] R. Aaij, et al. (LHCb), Measurements of the branching fractions of $\Lambda_c^+ \rightarrow p\pi^-\pi^+$, $\Lambda_c^+ \rightarrow pK^-K^+$, and $\Lambda_c^+ \rightarrow p\pi^-K^+$, JHEP 03 (2018) 043. doi:10.1007/JHEP03(2018)043. arXiv:1711.01157.
- [10] R. Aaij, et al. (LHCb), A measurement of the CP asymmetry difference in $\Lambda_c^+ \rightarrow pK^-K^+$ and $p\pi^-\pi^+$ decays, JHEP 03 (2018) 182. doi:10.1007/JHEP03(2018)182. arXiv:1712.07051.
- [11] R. Aaij, et al. (LHCb), Search for the rare decay $\Lambda_c^+ \rightarrow p\mu^+\mu^-$, Phys. Rev. D 97 (2018) 091101. doi:10.1103/PhysRevD.97.091101. arXiv:1712.07938.
- [12] R. Aaij, et al. (LHCb), Observation of the doubly Cabibbo-suppressed decay $\Xi_c^+ \rightarrow p\phi$, JHEP 04 (2019) 084. doi:10.1007/JHEP04(2019)084. arXiv:1901.06222.
- [13] R. Aaij, et al. (LHCb), Precision measurement of the Λ_c^+ , Ξ_c^+ and Ξ_c^0 baryon lifetimes, Phys. Rev. D 100 (2019) 032001. doi:10.1103/PhysRevD.100.032001. arXiv:1906.08350.
- [14] R. Aaij, et al. (LHCb), Search for CP violation in $\Xi_c^+ \rightarrow pK^-\pi^+$ decays using model-independent techniques, Eur. Phys. J. C 80 (2020) 986. doi:10.1140/epjc/s10052-020-8365-0. arXiv:2006.03145.
- [15] R. Aaij, et al. (LHCb), Amplitude analysis of the $\Lambda_c \rightarrow pK^-\pi^+$ decay and Λ_c baryon polarization measurement in semileptonic beauty hadron decays, Phys. Rev. D 108 (2023) 012023. doi:10.1103/PhysRevD.108.012023. arXiv:2208.03262.
- [16] R. Aaij, et al. (LHCb), Λ_c^+ polarimetry using the dominant hadronic mode, JHEP 07 (2023) 228. doi:10.1007/JHEP07(2023)228. arXiv:2301.07010.
- [17] S. B. Yang, et al. (Belle), First Observation of Doubly Cabibbo-Suppressed Decay of a Charmed Baryon: $\Lambda_c^+ \rightarrow pK^+\pi^-$, Phys. Rev. Lett. 117 (2016) 011801. doi:10.1103/PhysRevLett.117.011801. arXiv:1512.07366.
- [18] B. Pal, et al. (Belle), Search for $\Lambda_c^+ \rightarrow \phi p\pi^0$ and branching fraction measurement of $\Lambda_c^+ \rightarrow K^-\pi^+p\pi^0$, Phys. Rev. D 96 (2017) 051102. doi:10.1103/PhysRevD.96.051102. arXiv:1707.00089.
- [19] M. Berger, et al. (Belle), Measurement of the Decays $\Lambda_c \rightarrow \Sigma\pi$ at Belle, Phys. Rev. D 98 (2018) 112006. doi:10.1103/PhysRevD.98.112006. arXiv:1802.03421.
- [20] M. Sumihama, et al. (Belle), Observation of $\Xi(1620)^0$ and evidence for $\Xi(1690)^0$ in $\Xi_c^+ \rightarrow \Xi^-\pi^+\pi^+$ decays, Phys. Rev. Lett. 122 (2019) 072501. doi:10.1103/PhysRevLett.122.072501. arXiv:1810.06181.
- [21] Y. B. Li, et al. (Belle), First measurements of absolute branching fractions of the Ξ_c^+ baryon at Belle, Phys. Rev. D 100 (2019) 031101. doi:10.1103/PhysRevD.100.031101. arXiv:1904.12093.
- [22] J. Y. Lee, et al. (Belle), Measurement of branching fractions of $\Lambda_c^+ \rightarrow \eta\Lambda\pi^+$, $\eta\Sigma^0\pi^+$, $\Lambda(1670)\pi^+$, and $\eta\Sigma(1385)^+$, Phys. Rev. D 103 (2021) 052005. doi:10.1103/PhysRevD.103.052005. arXiv:2008.11575.
- [23] S. X. Li, et al. (Belle), Measurements of the branching fractions of $\Lambda_c^+ \rightarrow p\eta$ and $\Lambda_c^+ \rightarrow p\pi^0$ decays at Belle, Phys. Rev. D 103 (2021) 072004. doi:10.1103/PhysRevD.103.072004. arXiv:2102.12226.
- [24] Y. B. Li, et al. (Belle), Measurements of the branching fractions of the semileptonic decays $\Xi_c^0 \rightarrow \Xi^-\ell^+\nu_\ell$ and the asymmetry parameter of $\Xi_c^0 \rightarrow \Xi^-\pi^+$, Phys. Rev. Lett. 127 (2021) 121803. doi:10.

- 1103/PhysRevLett.127.121803. arXiv:2103.06496.
- [25] S. X. Li, et al. (Belle), Measurement of the branching fraction of $\Lambda_c^+ \rightarrow p\omega$ decay at Belle, Phys. Rev. D 104 (2021) 072008. doi:10.1103/PhysRevD.104.072008. arXiv:2108.11301.
- [26] Y. Li, et al. (Belle), Measurements of the branching fractions of $\Xi_c^0 \rightarrow \Lambda K_S^0$, $\Xi_c^0 \rightarrow \Sigma^0 K_S^0$, and $\Xi_c^0 \rightarrow \Sigma^+ K^-$ decays at Belle, Phys. Rev. D 105 (2022) L011102. doi:10.1103/PhysRevD.105.L011102. arXiv:2111.08981.
- [27] S. X. Li, et al. (Belle), First Measurement of the $\Lambda_c^+ \rightarrow p\eta'$ decay, JHEP 03 (2022) 090. doi:10.1007/JHEP03(2022)090. arXiv:2112.14276.
- [28] Y. Li, et al. (Belle), First search for the weak radiative decays $\Lambda c+ \rightarrow \Sigma + \gamma$ and $\Xi c0 \rightarrow \Xi 0 \gamma$, Phys. Rev. D 107 (2023) 032001. doi:10.1103/PhysRevD.107.032001. arXiv:2206.12517.
- [29] F. Abudinén, et al. (Belle-II), Measurement of the $\Lambda c+$ Lifetime, Phys. Rev. Lett. 130 (2023) 071802. doi:10.1103/PhysRevLett.130.071802. arXiv:2206.15227.
- [30] L. K. Li, et al. (Belle), Search for CP violation and measurement of branching fractions and decay asymmetry parameters for $\Lambda c+ \rightarrow \Lambda h+$ and $\Lambda c+ \rightarrow \Sigma 0 h+$ ($h=K, \pi$), Sci. Bull. 68 (2023) 583–592. doi:10.1016/j.scib.2023.02.017. arXiv:2208.08695.
- [31] S. X. Li, et al. (Belle), Measurements of branching fractions of $\Lambda_c^+ \rightarrow \Sigma^+ \eta$ and $\Lambda_c^+ \rightarrow \Sigma^+ \eta'$ and asymmetry parameters of $\Lambda_c^+ \rightarrow \Sigma^+ \pi^0$, $\Lambda_c^+ \rightarrow \Sigma^+ \eta$, and $\Lambda_c^+ \rightarrow \Sigma^+ \eta'$, Phys. Rev. D 107 (2023) 032003. doi:10.1103/PhysRevD.107.032003. arXiv:2208.10825.
- [32] S. B. Yang, et al. (Belle), Observation of a threshold cusp at the $\Lambda\eta$ threshold in the pK- mass spectrum with $\Lambda c+ \rightarrow pK-\pi+$ decays, Phys. Rev. D 108 (2023) L031104. doi:10.1103/PhysRevD.108.L031104. arXiv:2209.00050.
- [33] X. Han, et al. (Belle), Evidence for the singly Cabibbo-suppressed decay $\Omega_c^0 \rightarrow \Xi^- \pi^+$ and search for $\Omega_c^0 \rightarrow \Xi^- K^+$ and $\Omega^- K^+$ decays at Belle, JHEP 01 (2023) 055. doi:10.1007/JHEP01(2023)055. arXiv:2209.08583.
- [34] L. K. Li, et al. (Belle), Measurement of branching fractions of $\Lambda_c^+ \rightarrow pK_S^0 K_S^0$ and $\Lambda_c^+ \rightarrow pK_S^0 \eta$ at Belle, Phys. Rev. D 107 (2023) 032004. doi:10.1103/PhysRevD.107.032004. arXiv:2210.01995.
- [35] Y. Ma, et al. (Belle), First Observation of $\Lambda\pi+$ and $\Lambda\pi-$ Signals near the $K^- N(I=1)$ Mass Threshold in $\Lambda c+ \rightarrow \Lambda\pi+\pi+\pi-$ Decay, Phys. Rev. Lett. 130 (2023) 151903. doi:10.1103/PhysRevLett.130.151903. arXiv:2211.11151.
- [36] J. X. Cui, et al. (Belle), Search for the semileptonic decays $\Xi c0 \rightarrow \Xi 0 \ell+ \ell-$ at Belle, Phys. Rev. D 109 (2024) 052003. doi:10.1103/PhysRevD.109.052003. arXiv:2312.02580.
- [37] I. Adachi, et al. (Belle-II, Belle), Measurements of the branching fractions of $\Xi_c^0 \rightarrow \Xi^0 \pi^0$, $\Xi_c^0 \rightarrow \Xi^0 \eta$, and $\Xi_c^0 \rightarrow \Xi^0 \eta'$ and asymmetry parameter of $\Xi_c^0 \rightarrow \Xi^0 \pi^0$ (2024). arXiv:2406.04642.
- [38] M. Ablikim, et al. (BESIII), Measurement of the absolute branching fraction for $\Lambda_c^+ \rightarrow \Lambda e^+ \nu_e$, Phys. Rev. Lett. 115 (2015) 221805. doi:10.1103/PhysRevLett.115.221805. arXiv:1510.02610.
- [39] M. Ablikim, et al. (BESIII), Measurements of absolute hadronic branching fractions of Λ_c^+ baryon, Phys. Rev. Lett. 116 (2016) 052001. doi:10.1103/PhysRevLett.116.052001. arXiv:1511.08380.
- [40] M. Ablikim, et al. (BESIII), Measurement of Singly Cabibbo Suppressed Decays $\Lambda_c^+ \rightarrow p\pi^+\pi^-$ and $\Lambda_c^+ \rightarrow pK^+K^-$, Phys. Rev. Lett. 117 (2016) 232002. doi:10.1103/PhysRevLett.117.232002. arXiv:1608.00407, [Addendum: Phys.Rev.Lett. 120, 029903 (2018)].
- [41] M. Ablikim, et al. (BESIII), Observation of $\Lambda_c^+ \rightarrow nK_S^0 \pi^+$, Phys. Rev. Lett. 118 (2017) 112001. doi:10.1103/PhysRevLett.118.112001. arXiv:1611.02797.
- [42] M. Ablikim, et al. (BESIII), Evidence for the singly-Cabibbo-suppressed decay $\Lambda_c^+ \rightarrow p\eta$ and search for $\Lambda_c^+ \rightarrow p\pi^0$, Phys. Rev. D 95 (2017) 111102. doi:10.1103/PhysRevD.95.111102. arXiv:1702.05279.
- [43] M. Ablikim, et al. (BESIII), Observation of the decay $\Lambda_c^+ \rightarrow \Sigma^-\pi^+\pi^+\pi^0$, Phys. Lett. B 772 (2017) 388–393. doi:10.1016/j.physletb.2017.06.065. arXiv:1705.11109.
- [44] M. Ablikim, et al. (BESIII), Measurements of absolute branching fractions for $\Lambda_c^+ \rightarrow \Xi^0 K^+$ and $\Xi(1530)^0 K^+$, Phys. Lett. B 783 (2018) 200–206. doi:10.1016/j.physletb.2018.06.046. arXiv:1803.04299.
- [45] M. Ablikim, et al. (BESIII), Measurement of absolute branching fraction of the inclusive decay $\Lambda_c^+ \rightarrow \Lambda + X$, Phys. Rev. Lett. 121 (2018) 062003. doi:10.1103/PhysRevLett.121.062003. arXiv:1803.05706.
- [46] M. Ablikim, et al. (BESIII), Measurement of the absolute branching fraction of the inclusive semileptonic Λ_c^+ decay, Phys. Rev. Lett. 121 (2018) 251801. doi:10.1103/PhysRevLett.121.251801. arXiv:1805.09060.

- [47] M. Ablikim, et al. (BESIII), Evidence for the decays of $\Lambda_c^+ \rightarrow \Sigma^+\eta$ and $\Sigma^+\eta'$, Chin. Phys. C 43 (2019) 083002. doi:10.1088/1674-1137/43/8/083002. arXiv:1811.08028.
- [48] M. Ablikim, et al. (BESIII), Measurements of Weak Decay Asymmetries of $\Lambda_c^+ \rightarrow pK_S^0$, $\Lambda\pi^+$, $\Sigma^+\pi^0$, and $\Sigma^0\pi^+$, Phys. Rev. D 100 (2019) 072004. doi:10.1103/PhysRevD.100.072004. arXiv:1905.04707.
- [49] M. Ablikim, et al. (BESIII), Measurement of the absolute branching fraction of the inclusive decay $\Lambda_c^+ \rightarrow K_S^0 X$, Eur. Phys. J. C 80 (2020) 935. doi:10.1140/epjc/s10052-020-08447-0. arXiv:2005.11211.
- [50] M. Ablikim, et al. (BESIII), Measurement of the absolute branching fraction of $\Lambda_c^+ \rightarrow pK_S^0\eta$ decays, Phys. Lett. B 817 (2021) 136327. doi:10.1016/j.physletb.2021.136327. arXiv:2012.11106.
- [51] M. Ablikim, et al. (BESIII), Observation of the Singly Cabibbo Suppressed Decay $\Lambda_c^+ \rightarrow n\pi^+$, Phys. Rev. Lett. 128 (2022) 142001. doi:10.1103/PhysRevLett.128.142001. arXiv:2201.02056.
- [52] M. Ablikim, et al. (BESIII), Measurement of Branching Fractions of Singly Cabibbo-suppressed Decays $\Lambda_c^+ \rightarrow \Sigma^0 K^+$ and $\Sigma^+ K_S^0$, Phys. Rev. D 106 (2022) 052003. doi:10.1103/PhysRevD.106.052003. arXiv:2207.10906.
- [53] M. Ablikim, et al. (BESIII), First observation of the semileptonic decay $\Lambda c+ \rightarrow pK^-e^+\nu e$, Phys. Rev. D 106 (2022) 112010. doi:10.1103/PhysRevD.106.112010. arXiv:2207.11483.
- [54] M. Ablikim, et al. (BESIII), Measurement of the absolute branching fraction of the singly Cabibbo suppressed decay $\Lambda_c^+ \rightarrow p\eta'$, Phys. Rev. D 106 (2022) 072002. doi:10.1103/PhysRevD.106.072002. arXiv:2207.14461.
- [55] M. Ablikim, et al. (BESIII), Study of the Semileptonic Decay $\Lambda c+ \rightarrow \Lambda e^+\nu e$, Phys. Rev. Lett. 129 (2022) 231803. doi:10.1103/PhysRevLett.129.231803. arXiv:2207.14149.
- [56] M. Ablikim, et al. (BESIII), Search for a massless dark photon in $\Lambda c+ \rightarrow p\gamma'$ decay, Phys. Rev. D 106 (2022) 072008. doi:10.1103/PhysRevD.106.072008. arXiv:2208.04496.
- [57] M. Ablikim, et al. (BESIII), Measurement of the branching fraction of the singly Cabibbo-suppressed decay $\Lambda c+ \rightarrow \Lambda K^+$, Phys. Rev. D 106 (2022) L111101. doi:10.1103/PhysRevD.106.L111101. arXiv:2208.04001.
- [58] M. Ablikim, et al. (BESIII), Partial wave analysis of the charmed baryon hadronic decay $\Lambda_c^+ \rightarrow \Lambda\pi^+\pi^0$, JHEP 12 (2022) 033. doi:10.1007/JHEP12(2022)033. arXiv:2209.08464.
- [59] M. Ablikim, et al. ((BESIII), BESIII), Observations of the Cabibbo-Suppressed decays $\Lambda_c^+ \rightarrow n\pi^+\pi^0$, $n\pi^+\pi^-\pi^+$ and the Cabibbo-Favored decay $\Lambda_c^+ \rightarrow nK^-\pi^+\pi^+$, Chin. Phys. C 47 (2023) 023001. doi:10.1088/1674-1137/ac9d29. arXiv:2210.03375.
- [60] M. Ablikim, et al. (BESIII), Improved measurement of the absolute branching fraction of inclusive semileptonic $\Lambda c+$ decay, Phys. Rev. D 107 (2023) 052005. doi:10.1103/PhysRevD.107.052005. arXiv:2212.03753.
- [61] M. Ablikim, et al. (BESIII), Search for the weak radiative decay $\Lambda c+ \rightarrow \Sigma+\gamma$ at BESIII, Phys. Rev. D 107 (2023) 052002. doi:10.1103/PhysRevD.107.052002. arXiv:2212.07214.
- [62] M. Ablikim, et al. (BESIII), Search for the semi-leptonic decays $\Lambda c+ \rightarrow \Lambda\pi^+\pi^-e^+\nu e$ and $\Lambda c+ \rightarrow pKS0\pi^-e^+\nu e$, Phys. Lett. B 843 (2023) 137993. doi:10.1016/j.physletb.2023.137993. arXiv:2302.07529.
- [63] M. Ablikim, et al. (BESIII), Measurement of branching fractions of Λ_c^+ decays to $\Sigma^+K^+K^-$, $\Sigma^+\phi$ and $\Sigma^+K^+\pi^-(\pi^0)$, JHEP 09 (2023) 125. doi:10.1007/JHEP09(2023)125. arXiv:2304.09405.
- [64] M. Ablikim, et al. (BESIII), Study of $\Lambda_c^+ \rightarrow \Lambda\mu^+\nu_\mu$ and test of lepton flavor universality with $\Lambda_c^+ \rightarrow \Lambda\ell^+\nu_\ell$ decays, Phys. Rev. D 108 (2023) L031105. doi:10.1103/PhysRevD.108.L031105. arXiv:2306.02624.
- [65] M. Ablikim, et al. (BESIII), Measurement of the branching fractions of the singly Cabibbo-suppressed decays $\Lambda_c^+ \rightarrow p\eta$ and $\Lambda_c^+ \rightarrow p\omega$, JHEP 11 (2023) 137. doi:10.1007/JHEP11(2023)137. arXiv:2307.09266.
- [66] M. Ablikim, et al. (BESIII), Study of $\Lambda_c^+ \rightarrow \Lambda\mu^+\nu_\mu$ and test of lepton flavor universality with $\Lambda_c^+ \rightarrow \Lambda\ell^+\nu_\ell$ decays, Phys. Rev. D 108 (2023) L031105. doi:10.1103/PhysRevD.108.L031105. arXiv:2306.02624.
- [67] M. Ablikim, et al. (BESIII), First Measurement of the Decay Asymmetry in the Pure W-Boson-Exchange Decay $\Lambda c+ \rightarrow \Xi0K^+$, Phys. Rev. Lett. 132 (2024) 031801. doi:10.1103/PhysRevLett.132.031801. arXiv:2309.02774.
- [68] M. Ablikim, et al. (BESIII), Observation of the singly Cabibbo-suppressed decay $\Lambda c+ \rightarrow \Sigma^-K^+\pi^+$, Phys. Rev. D 109 (2024) L071103. doi:10.1103/PhysRevD.109.L071103. arXiv:2309.05484.

- [69] M. Ablikim, et al. (BESIII), Measurement of the absolute branching fraction of the three-body decay $\Lambda c \rightarrow \Xi 0 K + \pi 0$ and search for $\Lambda c \rightarrow n K + \pi 0$, $\Sigma 0 K + \pi 0$, and $\Lambda K + \pi 0$, Phys. Rev. D 109 (2024) 052001. doi:10.1103/PhysRevD.109.052001. arXiv:2311.02347.
- [70] M. Ablikim, et al. (BESIII), Evidence of the singly Cabibbo suppressed decay $\Lambda c \rightarrow p \pi 0$, Phys. Rev. D 109 (2024) L091101. doi:10.1103/PhysRevD.109.L091101. arXiv:2311.06883.
- [71] M. Ablikim, et al. (BESIII), First observation of $\Lambda c \rightarrow \Lambda K + \pi 0$ and evidence of $\Lambda c \rightarrow \Lambda K + \pi + \pi -$, Phys. Rev. D 109 (2024) 032003. doi:10.1103/PhysRevD.109.032003. arXiv:2311.12903.
- [72] M. Ablikim, et al. (BESIII), Measurement of branching fractions for $\Lambda c \rightarrow n K S 0 \pi +$ and $\Lambda c \rightarrow n K S 0 K +$, Phys. Rev. D 109 (2024) 072010. doi:10.1103/PhysRevD.109.072010. arXiv:2311.17131.
- [73] M. Ablikim, et al. (BESIII), First observation of the decay $\Lambda c \rightarrow n K S 0 \pi + \pi 0$, Phys. Rev. D 109 (2024) 053005. doi:10.1103/PhysRevD.109.053005. arXiv:2401.06813.
- [74] M. Ablikim, et al. (BESIII), Measurements of $K_S^0 - K_L^0$ asymmetries in the decays $\Lambda_c^+ \rightarrow p K_{L,S}^0$, $p K_{L,S}^0 \pi^+ \pi^-$ and $p K_{L,S}^0 \pi^0$ (2024). arXiv:2406.18083.
- [75] M. Ablikim, et al. (BESIII), Observation of $\Lambda_c^+ \rightarrow \Lambda a_0(980)^+$ and Evidence for $\Sigma(1380)^+$ in $\Lambda_c^+ \rightarrow \Lambda \pi^+ \eta$ (2024). arXiv:2407.12270.
- [76] M. J. Savage, SU(3) violations in the nonleptonic decay of charmed hadrons, Phys. Lett. B 257 (1991) 414–418. doi:10.1016/0370-2693(91)91917-K.
- [77] S. M. Sheikhholeslami, M. P. Khanna, R. C. Verma, Cabibbo enhanced weak decays of charmed baryons in the SU(4) semidynamical scheme, Phys. Rev. D 43 (1991) 170–178. doi:10.1103/PhysRevD.43.170.
- [78] R. C. Verma, M. P. Khanna, Cabibbo favored hadronic decays of charmed baryons in flavor SU(3), Phys. Rev. D 53 (1996) 3723–3730. doi:10.1103/PhysRevD.53.3723. arXiv:hep-ph/9506394.
- [79] K. K. Sharma, R. C. Verma, SU(3) flavor analysis of two-body weak decays of charmed baryons, Phys. Rev. D 55 (1997) 7067–7074. doi:10.1103/PhysRevD.55.7067. arXiv:hep-ph/9704391.
- [80] S.-L. Chen, X.-H. Guo, X.-Q. Li, G.-L. Wang, Cabibbo suppressed nonleptonic decays of Lambda(c) and final state interaction, Commun. Theor. Phys. 40 (2003) 563–572. doi:10.1088/0253-6102/40/5/563. arXiv:hep-ph/0208006.
- [81] C.-D. Lü, W. Wang, F.-S. Yu, Test flavor SU(3) symmetry in exclusive Λ_c decays, Phys. Rev. D 93 (2016) 056008. doi:10.1103/PhysRevD.93.056008. arXiv:1601.04241.
- [82] D. Wang, P.-F. Guo, W.-H. Long, F.-S. Yu, $K_S^0 - K_L^0$ asymmetries and CP violation in charmed baryon decays into neutral kaons, JHEP 03 (2018) 066. doi:10.1007/JHEP03(2018)066. arXiv:1709.09873.
- [83] C. Q. Geng, Y. K. Hsiao, Y.-H. Lin, L.-L. Liu, Non-leptonic two-body weak decays of $\Lambda_c(2286)$, Phys. Lett. B 776 (2018) 265–269. doi:10.1016/j.physletb.2017.11.062. arXiv:1708.02460.
- [84] C. Q. Geng, Y. K. Hsiao, C.-W. Liu, T.-H. Tsai, Charmed Baryon Weak Decays with SU(3) Flavor Symmetry, JHEP 11 (2017) 147. doi:10.1007/JHEP11(2017)147. arXiv:1709.00808.
- [85] H.-Y. Cheng, X.-W. Kang, F. Xu, Singly Cabibbo-suppressed hadronic decays of Λ_c^+ , Phys. Rev. D 97 (2018) 074028. doi:10.1103/PhysRevD.97.074028. arXiv:1801.08625.
- [86] J. Zou, F. Xu, G. Meng, H.-Y. Cheng, Two-body hadronic weak decays of antitriplet charmed baryons, Phys. Rev. D 101 (2020) 014011. doi:10.1103/PhysRevD.101.014011. arXiv:1910.13626.
- [87] C.-P. Jia, D. Wang, F.-S. Yu, Charmed baryon decays in $SU(3)_F$ symmetry, Nucl. Phys. B 956 (2020) 115048. doi:10.1016/j.nuclphysb.2020.115048. arXiv:1910.00876.
- [88] Y. K. Hsiao, Y. Yao, H. J. Zhao, Two-body charmed baryon decays involving vector meson with $SU(3)$ flavor symmetry, Phys. Lett. B 792 (2019) 35–39. doi:10.1016/j.physletb.2019.03.031. arXiv:1902.08783.
- [89] C. Q. Geng, C.-W. Liu, T.-H. Tsai, Asymmetries of anti-triplet charmed baryon decays, Phys. Lett. B 794 (2019) 19–28. doi:10.1016/j.physletb.2019.05.024. arXiv:1902.06189.
- [90] J.-Y. Cen, C.-Q. Geng, C.-W. Liu, T.-H. Tsai, Up-down asymmetries of charmed baryon three-body decays, Eur. Phys. J. C 79 (2019) 946. doi:10.1140/epjc/s10052-019-7467-z. arXiv:1906.01848.
- [91] G. Meng, S. M.-Y. Wong, F. Xu, Doubly Cabibbo-suppressed decays of antitriplet charmed baryons, JHEP 11 (2020) 126. doi:10.1007/JHEP11(2020)126. arXiv:2005.12111.
- [92] C. Q. Geng, C.-W. Liu, T.-H. Tsai, Charmed Baryon Weak Decays with Vector Mesons, Phys. Rev. D 101 (2020) 053002. doi:10.1103/PhysRevD.101.053002. arXiv:2001.05079.
- [93] C. Q. Geng, C.-W. Liu, T.-H. Tsai, Mixing effects of $\Sigma^0 - \Lambda^0$ in Λ_c^+ decays, Phys. Rev. D 101 (2020) 054005. doi:10.1103/PhysRevD.101.054005. arXiv:2002.09583.
- [94] H.-W. Ke, X.-Q. Li, A natural interpretation on the data of $\Lambda_c \rightarrow \Sigma \pi$, Phys. Rev. D 102 (2020)

113013. doi:10.1103/PhysRevD.102.113013. arXiv:2008.12163.
- [95] Y.-S. Li, X. Liu, F.-S. Yu, Revisiting semileptonic decays of $\Lambda_{b(c)}$ supported by baryon spectroscopy, Phys. Rev. D 104 (2021) 013005. doi:10.1103/PhysRevD.104.013005. arXiv:2104.04962.
- [96] F. Xu, Q. Wen, H. Zhong, $K_S^0 - K_L^0$ Asymmetries in Weak Decays of Charmed Baryons, LHEP 2021 (2021) 218. doi:10.31526/1hep.2021.218.
- [97] Y. K. Hsiao, Y. L. Wang, H. J. Zhao, Equivalent $SU(3)_f$ approaches for two-body anti-triplet charmed baryon decays, JHEP 09 (2022) 035. doi:10.1007/JHEP09(2022)035. arXiv:2111.04124.
- [98] J.-P. Wang, F.-S. Yu, Probing hyperon CP violation with charmed baryon decays, Phys. Lett. B 849 (2024) 138460. doi:10.1016/j.physletb.2024.138460. arXiv:2208.01589.
- [99] H.-Y. Cheng, F. Xu, Heavy-flavor-conserving hadronic weak decays of charmed and bottom baryons, Phys. Rev. D 105 (2022) 094011. doi:10.1103/PhysRevD.105.094011. arXiv:2204.03149.
- [100] H. Zhong, F. Xu, Q. Wen, Y. Gu, Weak decays of antitriplet charmed baryons from the perspective of flavor symmetry, JHEP 02 (2023) 235. doi:10.1007/JHEP02(2023)235. arXiv:2210.12728.
- [101] H. Liu, C. Yang, Two-body hadronic decays of $\Xi c 0$ in light front approach, Phys. Rev. D 108 (2023) 093011. doi:10.1103/PhysRevD.108.093011. arXiv:2304.12128.
- [102] Z.-P. Xing, X.-G. He, F. Huang, C. Yang, Global analysis of measured and unmeasured hadronic two-body weak decays of antitriplet charmed baryons, Phys. Rev. D 108 (2023) 053004. doi:10.1103/PhysRevD.108.053004. arXiv:2305.14854.
- [103] C.-W. Liu, Nonleptonic two-body weak decays of charmed baryons, Phys. Rev. D 109 (2024) 033004. doi:10.1103/PhysRevD.109.033004. arXiv:2308.07754.
- [104] Z.-P. Xing, X.-G. He, F. Huang, C. Yang, Global analysis of measured and unmeasured hadronic two-body weak decays of antitriplet charmed baryons, Phys. Rev. D 108 (2023) 053004. doi:10.1103/PhysRevD.108.053004. arXiv:2305.14854.
- [105] C.-Q. Geng, X.-G. He, X.-N. Jin, C.-W. Liu, C. Yang, Complete determination of $SU(3)_F$ amplitudes and strong phase in $\Lambda c \rightarrow \Xi 0 K^+$, Phys. Rev. D 109 (2024) L071302. doi:10.1103/PhysRevD.109.L071302. arXiv:2310.05491.
- [106] Y.-J. Shi, Z.-X. Zhao, Light-cone sum rules study on the purely non-factorizable $\Lambda_c^+ \rightarrow \Xi^0 K^+$ decay (2024). arXiv:2407.07431.
- [107] H. Zhong, F. Xu, H.-Y. Cheng, Topological Diagrams and Hadronic Weak Decays of Charmed Baryons (2024). arXiv:2401.15926.
- [108] H. Zhong, F. Xu, H.-Y. Cheng, Analysis of hadronic weak decays of charmed baryons in the topological diagrammatic approach, Phys. Rev. D 109 (2024) 114027. doi:10.1103/PhysRevD.109.114027. arXiv:2404.01350.
- [109] C.-Q. Geng, C.-W. Liu, S.-L. Liu, Nonleptonic three-body charmed baryon weak decays with $H(15)$, Phys. Rev. D 109 (2024) 093002. doi:10.1103/PhysRevD.109.093002. arXiv:2403.06469.
- [110] D. Wang, J.-F. Luo, Topological amplitudes of charmed baryon decays in the $SU(3)_F$ limit (2024). arXiv:2406.14061.
- [111] D. Wang, Topological diagram analysis of $\mathcal{B}_{c\bar{3}} \rightarrow \mathcal{B}_{10} M$ decays in the $SU(3)_F$ limit and beyond (2024). arXiv:2408.02015.
- [112] Y. Grossman, S. Schacht, U-Spin Sum Rules for CP Asymmetries of Three-Body Charmed Baryon Decays, Phys. Rev. D 99 (2019) 033005. doi:10.1103/PhysRevD.99.033005. arXiv:1811.11188.
- [113] D. Wang, Sum rules for CP asymmetries of charmed baryon decays in the $SU(3)_F$ limit, Eur. Phys. J. C 79 (2019) 429. doi:10.1140/epjc/s10052-019-6925-y. arXiv:1901.01776.
- [114] X.-G. He, C.-W. Liu, Large CP violation in charmed baryon decays (2024). arXiv:2404.19166.
- [115] J. Sun, R. Zhu, Z.-P. Xing, Observable CP-violation in charmed baryons decays with $SU(3)$ symmetry analysis (2024). arXiv:2407.00426.
- [116] Z.-P. Xing, Y.-J. Shi, J. Sun, Y. Xing, $SU(3)$ symmetry analysis in charmed baryon two body decays with penguin diagram contribution (2024). arXiv:2407.09234.
- [117] J. G. Körner, G. Kramer, J. Willrodt, Weak Decays of the Charmed Baryon C_0^+ and the Inclusive Yield of Λ and p , Phys. Lett. B 78 (1978) 492. doi:10.1016/0370-2693(78)90495-1, [Erratum: Phys.Lett.B 81, 419–419 (1979)].
- [118] Y. Kohara, Quark diagram analysis of charmed baryon decays, Phys. Rev. D 44 (1991) 2799–2802. doi:10.1103/PhysRevD.44.2799.
- [119] H.-Y. Cheng, B. Tseng, Nonleptonic weak decays of charmed baryons, Phys. Rev. D 46 (1992) 1042. doi:10.1103/PhysRevD.46.1042, [Erratum: Phys.Rev.D 55, 1697 (1997)].

- [120] J. G. Korner, M. Kramer, Exclusive nonleptonic charm baryon decays, *Z. Phys. C* 55 (1992) 659–670. doi:10.1007/BF01561305.
- [121] Q. P. Xu, A. N. Kamal, Cabibbo favored nonleptonic decays of charmed baryons, *Phys. Rev. D* 46 (1992) 270–278. doi:10.1103/PhysRevD.46.270.
- [122] Q. P. Xu, A. N. Kamal, The Nonleptonic charmed baryon decays: $B(c) \rightarrow B(3/2+, \text{decuplet}) + P(0-) \text{ or } V(1-)$, *Phys. Rev. D* 46 (1992) 3836–3844. doi:10.1103/PhysRevD.46.3836.
- [123] P. Zenczykowski, Nonleptonic charmed baryon decays: Symmetry properties of parity violating amplitudes, *Phys. Rev. D* 50 (1994) 5787–5792. doi:10.1103/PhysRevD.50.5787.
- [124] H.-Y. Cheng, B. Tseng, Cabibbo allowed nonleptonic weak decays of charmed baryons, *Phys. Rev. D* 48 (1993) 4188–4202. doi:10.1103/PhysRevD.48.4188. arXiv:hep-ph/9304286.
- [125] T. Uppal, R. C. Verma, M. P. Khanna, Constituent quark model analysis of weak mesonic decays of charm baryons, *Phys. Rev. D* 49 (1994) 3417–3425. doi:10.1103/PhysRevD.49.3417.
- [126] L.-L. Chau, H.-Y. Cheng, B. Tseng, Analysis of two-body decays of charmed baryons using the quark diagram scheme, *Phys. Rev. D* 54 (1996) 2132–2160. doi:10.1103/PhysRevD.54.2132. arXiv:hep-ph/9508382.
- [127] M. A. Ivanov, J. G. Korner, V. E. Lyubovitskij, A. G. Rusetsky, Exclusive nonleptonic decays of bottom and charm baryons in a relativistic three quark model: Evaluation of nonfactorizing diagrams, *Phys. Rev. D* 57 (1998) 5632–5652. doi:10.1103/PhysRevD.57.5632. arXiv:hep-ph/9709372.
- [128] K. K. Sharma, R. C. Verma, A Study of weak mesonic decays of Lambda(c) and Xi(c) baryons on the basis of HQET results, *Eur. Phys. J. C* 7 (1999) 217–224. doi:10.1007/s100529801008. arXiv:hep-ph/9803302.
- [129] T. Gutsche, M. A. Ivanov, J. G. Körner, V. E. Lyubovitskij, Nonleptonic two-body decays of single heavy baryons Λ_Q , Ξ_Q , and Ω_Q ($Q = b, c$) induced by W emission in the covariant confined quark model, *Phys. Rev. D* 98 (2018) 074011. doi:10.1103/PhysRevD.98.074011. arXiv:1806.11549.
- [130] P.-Y. Niu, J.-M. Richard, Q. Wang, Q. Zhao, Hadronic weak decays of Λ_c in the quark model, *Phys. Rev. D* 102 (2020) 073005. doi:10.1103/PhysRevD.102.073005. arXiv:2003.09323.
- [131] R. Aaij, et al. (LHCb), Observation of CP Violation in Charm Decays, *Phys. Rev. Lett.* 122 (2019) 211803. doi:10.1103/PhysRevLett.122.211803. arXiv:1903.08726.
- [132] H.-n. Li, C.-D. Lu, F.-S. Yu, Branching ratios and direct CP asymmetries in $D \rightarrow PP$ decays, *Phys. Rev. D* 86 (2012) 036012. doi:10.1103/PhysRevD.86.036012. arXiv:1203.3120.
- [133] H.-N. Li, C.-D. Lü, F.-S. Yu, Implications on the first observation of charm CPV at LHCb (2019). arXiv:1903.10638.
- [134] I. Bediaga, T. Frederico, P. C. Magalhães, Enhanced Charm CP Asymmetries from Final State Interactions, *Phys. Rev. Lett.* 131 (2023) 051802. doi:10.1103/PhysRevLett.131.051802. arXiv:2203.04056.
- [135] A. Pich, E. Solomonidi, L. Vale Silva, Final-state interactions in the CP asymmetries of charm-meson two-body decays, *Phys. Rev. D* 108 (2023) 036026. doi:10.1103/PhysRevD.108.036026. arXiv:2305.11951.
- [136] H.-Y. Cheng, C.-K. Chua, A. Soni, Final state interactions in hadronic B decays, *Phys. Rev. D* 71 (2005) 014030. doi:10.1103/PhysRevD.71.014030. arXiv:hep-ph/0409317.
- [137] F.-S. Yu, H.-Y. Jiang, R.-H. Li, C.-D. Lü, W. Wang, Z.-X. Zhao, Discovery Potentials of Doubly Charmed Baryons, *Chin. Phys. C* 42 (2018) 051001. doi:10.1088/1674-1137/42/5/051001. arXiv:1703.09086.
- [138] L.-L. Chau, Quark Mixing in Weak Interactions, *Phys. Rept.* 95 (1983) 1–94. doi:10.1016/0370-1573(83)90043-1.
- [139] L. L. Chau, H. Y. Cheng, Quark Diagram Analysis of Two-body Charm Decays, *Phys. Rev. Lett.* 56 (1986) 1655–1658. doi:10.1103/PhysRevLett.56.1655.
- [140] M. Biyajima, K. Shirane, O. Terazawa, CALCULATIONS OF STANDARD HIGGS BOSON PRODUCTION CROSS-SECTIONS IN $E^+ E^-$ COLLISIONS BY MEANS OF A REASONABLE SET OF PARAMETERS. (REVISED VERSION), *Phys. Rev. D* 36 (1987) 2161–2164. doi:10.1103/PhysRevD.36.2161.
- [141] L.-L. Chau, H.-Y. Cheng, Comments on QCD Sum Rule Calculations of Exclusive Two-body Decays of Charmed Mesons, *Mod. Phys. Lett. A* 4 (1989) 877. doi:10.1142/S0217732389001039.
- [142] Y. Fu-Sheng, X.-X. Wang, C.-D. Lu, Nonleptonic Two Body Decays of Charmed Mesons, *Phys. Rev. D* 84 (2011) 074019. doi:10.1103/PhysRevD.84.074019. arXiv:1101.4714.

- [143] Q. Qin, H.-n. Li, C.-D. Lü, F.-S. Yu, Branching ratios and direct CP asymmetries in $D \rightarrow PV$ decays, Phys. Rev. D 89 (2014) 054006. doi:10.1103/PhysRevD.89.054006. arXiv:1305.7021.
- [144] J.-J. Han, H.-Y. Jiang, W. Liu, Z.-J. Xiao, F.-S. Yu, Rescattering mechanism of weak decays of double-charm baryons, Chin. Phys. C 45 (2021) 053105. doi:10.1088/1674-1137/abec68. arXiv:2101.12019.
- [145] J.-J. Han, R.-X. Zhang, H.-Y. Jiang, Z.-J. Xiao, F.-S. Yu, Weak decays of bottom-charm baryons: $\mathcal{B}_{bc} \rightarrow \mathcal{B}_b P$, Eur. Phys. J. C 81 (2021) 539. doi:10.1140/epjc/s10052-021-09239-w. arXiv:2102.00961.
- [146] A. K. Leibovich, Z. Ligeti, I. W. Stewart, M. B. Wise, Predictions for nonleptonic Lambda(b) and Theta(b) decays, Phys. Lett. B 586 (2004) 337–344. doi:10.1016/j.physletb.2004.02.033. arXiv:hep-ph/0312319.
- [147] S. Mantry, D. Pirjol, I. W. Stewart, Strong phases and factorization for color suppressed decays, Phys. Rev. D 68 (2003) 114009. doi:10.1103/PhysRevD.68.114009. arXiv:hep-ph/0306254.
- [148] H.-Y. Cheng, Nonleptonic weak decays of bottom baryons, Phys. Rev. D 56 (1997) 2799–2811. doi:10.1103/PhysRevD.56.2799. arXiv:hep-ph/9612223, [Erratum: Phys.Rev.D 99, 079901 (2019)].
- [149] L. Wolfenstein, Final state interactions and CP violation in weak decays, Phys. Rev. D 43 (1991) 151–156. doi:10.1103/PhysRevD.43.151.
- [150] M. Suzuki, L. Wolfenstein, Final state interaction phase in B decays, Phys. Rev. D 60 (1999) 074019. doi:10.1103/PhysRevD.60.074019. arXiv:hep-ph/9903477.
- [151] H.-Y. Cheng, C.-K. Chua, Branching fractions and CP violation in $B^- \rightarrow K^+ K^- \pi^-$ and $B^- \rightarrow \pi^+ \pi^- \pi^-$ decays, Phys. Rev. D 102 (2020) 053006. doi:10.1103/PhysRevD.102.053006. arXiv:2007.02558.
- [152] C.-K. Chua, Rescattering effects in charmless anti-B(u,d,s) $\rightarrow P P$ decays, Phys. Rev. D 78 (2008) 076002. doi:10.1103/PhysRevD.78.076002. arXiv:0712.4187.
- [153] J. P. Dedonder, A. Furman, R. Kaminski, L. Lesniak, B. Loiseau, S-, P- and D-wave final state interactions and CP violation in $B^{+-} \rightarrow \pi^+ \pi^- \pi^-$ decays, Acta Phys. Polon. B 42 (2011) 2013. doi:10.5506/APhysPolB.42.2013. arXiv:1011.0960.
- [154] I. Bediaga, T. Frederico, O. Lourenço, CP violation and CPT invariance in B^\pm decays with final state interactions, Phys. Rev. D 89 (2014) 094013. doi:10.1103/PhysRevD.89.094013. arXiv:1307.8164.
- [155] H.-Y. Cheng, C.-K. Chua, Branching Fractions and Direct CP Violation in Charmless Three-body Decays of B Mesons, Phys. Rev. D 88 (2013) 114014. doi:10.1103/PhysRevD.88.114014. arXiv:1308.5139.
- [156] F. Buccella, A. Paul, P. Santorelli, $SU(3)_F$ breaking through final state interactions and CP asymmetries in $D \rightarrow PP$ decays, Phys. Rev. D 99 (2019) 113001. doi:10.1103/PhysRevD.99.113001. arXiv:1902.05564.
- [157] H.-Y. Cheng, C.-W. Chiang, Two-body hadronic charmed meson decays, Phys. Rev. D 81 (2010) 074021. doi:10.1103/PhysRevD.81.074021. arXiv:1001.0987.
- [158] P. C. Magalhaes, M. R. Robilotta, K. S. F. Guimaraes, T. Frederico, W. de Paula, I. Bediaga, A. C. d. Reis, C. M. Maekawa, G. R. S. Zarnauskas, Towards three-body unitarity in $D^+ \rightarrow K^- \pi^+ \pi^+$, Phys. Rev. D 84 (2011) 094001. doi:10.1103/PhysRevD.84.094001. arXiv:1105.5120.
- [159] R. A. Garrote, J. Cuervo, P. C. Magalhães, J. R. Peláez, Dispersive $\pi\pi \rightarrow KK^-$ Amplitude and Giant CP Violation in B to Three Light-Meson Decays at LHCb, Phys. Rev. Lett. 130 (2023) 201901. doi:10.1103/PhysRevLett.130.201901. arXiv:2210.08354.
- [160] Y. Zhou, Imaginary part of Feynman amplitude, cutting rules and optical theorem (2004). arXiv:hep-ph/0412204.
- [161] A. Aste, Finite Quantum Electrodynamics, the Causal Approach, Annals of Physics 257 (1997,2nd ed., Springer, Berlin/Heidelberg/New York) 158.
- [162] O. Gortchakov, M. P. Locher, V. E. Markushin, S. von Rotz, Two meson doorway calculation for anti-p p $\rightarrow \phi \pi$ including off-shell effects and the OZI rule, Z. Phys. A 353 (1996) 447–453. doi:10.1007/BF01285155.
- [163] R. L. Workman, et al. (Particle Data Group), Review of Particle Physics, PTEP 2022 (2022) 083C01. doi:10.1093/ptep/ptac097.
- [164] P. Ball, G. W. Jones, R. Zwicky, $B \rightarrow V\gamma$ beyond QCD factorisation, Phys. Rev. D 75 (2007) 054004. doi:10.1103/PhysRevD.75.054004. arXiv:hep-ph/0612081.
- [165] W. Detmold, S. Meinel, $\Lambda_b \rightarrow \Lambda \ell^+ \ell^-$ form factors, differential branching fraction, and angular

- observables from lattice QCD with relativistic b quarks, Phys. Rev. D 93 (2016) 074501. doi:10.1103/PhysRevD.93.074501. arXiv:1602.01399.
- [166] S. Meinel, $\Lambda_c \rightarrow \Lambda l^+ \nu_l$ form factors and decay rates from lattice QCD with physical quark masses, Phys. Rev. Lett. 118 (2017) 082001. doi:10.1103/PhysRevLett.118.082001. arXiv:1611.09696.
- [167] S. Meinel, $\Lambda_c \rightarrow N$ form factors from lattice QCD and phenomenology of $\Lambda_c \rightarrow n l^+ \nu_\ell$ and $\Lambda_c \rightarrow p \mu^+ \mu^-$ decays, Phys. Rev. D 97 (2018) 034511. doi:10.1103/PhysRevD.97.034511. arXiv:1712.05783.
- [168] H. Bahtiyar, $\Lambda_c \rightarrow \Lambda$ Form Factors in Lattice QCD, Turk. J. Phys. 45 (2021) 4. doi:10.3906/fiz-2104-28. arXiv:2107.13909.
- [169] Z.-X. Zhao, Weak decays of heavy baryons in the light-front approach, Chin. Phys. C 42 (2018) 093101. doi:10.1088/1674-1137/42/9/093101. arXiv:1803.02292.
- [170] Y.-L. Liu, M.-Q. Huang, D.-W. Wang, Improved analysis on the semi-leptonic decay Lambda(c) —> Lambda l+ nu from QCD light-cone sum rules, Phys. Rev. D 80 (2009) 074011. doi:10.1103/PhysRevD.80.074011. arXiv:0910.1160.
- [171] T. Gutsche, M. A. Ivanov, J. G. Korner, V. E. Lyubovitskij, P. Santorelli, Semileptonic decays $\Lambda_c^+ \rightarrow \Lambda l^+ \nu_\ell$ ($\ell = e, \mu$) in the covariant quark model and comparison with the new absolute branching fraction measurements of Belle and BESIII, Phys. Rev. D 93 (2016) 034008. doi:10.1103/PhysRevD.93.034008. arXiv:1512.02168.
- [172] R. N. Faustov, V. O. Galkin, Rare $\Lambda_c \rightarrow p \ell^+ \ell^-$ decay in the relativistic quark model, Eur. Phys. J. C 78 (2018) 527. doi:10.1140/epjc/s10052-018-6010-y. arXiv:1805.02516.
- [173] T. M. Aliev, A. Ozpineci, S. B. Yakovlev, V. Zamiralov, Meson-octet-baryon couplings using light cone QCD sum rules, Phys. Rev. D 74 (2006) 116001. doi:10.1103/PhysRevD.74.116001.
- [174] T. M. Aliev, A. Ozpineci, M. Savci, V. S. Zamiralov, Vector meson-baryon strong coupling constants in light cone QCD sum rules, Phys. Rev. D 80 (2009) 016010. doi:10.1103/PhysRevD.80.016010. arXiv:0905.4664.
- [175] G. Janssen, K. Holinde, J. Speth, pi rho correlations in the N N potential, Phys. Rev. C 54 (1996) 2218–2234. doi:10.1103/PhysRevC.54.2218.
- [176] E. Oset, A. Ramos, Dynamically generated resonances from the vector octet-baryon octet interaction, Eur. Phys. J. A 44 (2010) 445–454. doi:10.1140/epja/i2010-10957-3. arXiv:0905.0973.
- [177] A. Bramon, A. Grau, G. Pancheri, Radiative vector meson decays in SU(3) broken effective chiral Lagrangians, Phys. Lett. B 344 (1995) 240–244. doi:10.1016/0370-2693(94)01543-L.
- [178] R. Aaij, et al. (LHCb), Search for the rare $\Lambda_c^+ \rightarrow p \mu^+ \mu^-$ decay (2024). arXiv:2407.11474.
- [179] P.-C. Hong, F. Yan, R.-G. Ping, T. Luo, Study of parity violation in and decays*, Chin. Phys. C 47 (2023) 053101. doi:10.1088/1674-1137/acb7ce. arXiv:2211.16014.
- [180] S. Fajfer, A. Prapotnik, P. Singer, J. Zupan, Final state interactions in the D+(s) —> omega pi+ and D+(s) —> rho0 pi+ decays, Phys. Rev. D 68 (2003) 094012. doi:10.1103/PhysRevD.68.094012. arXiv:hep-ph/0308100.
- [181] D. Ronchen, M. Doring, F. Huang, H. Haberzettl, J. Haidenbauer, C. Hanhart, S. Krewald, U. G. Meissner, K. Nakayama, Coupled-channel dynamics in the reactions piN —> piN, etaN, KLambda, KSigma, Eur. Phys. J. A 49 (2013) 44. doi:10.1140/epja/i2013-13044-5. arXiv:1211.6998.